INFLUENCE OF RING STIFFENERS AND PREBUCKLING DEFORMATIONS ON THE BUCKLING OF ECCENTRICALLY STIFFENED ORTHOTROPIC CYLINDERS

By

David L. Block

Thesis submitted to the Graduate Faculty of the

Virginia Polytechnic Institute

in candidacy for the degree of

DOCTOR OF PHILOSOPHY

in

ENGINEERING MECHANICS

June 1966

INFLUENCE OF RING STIFFENERS AND PREBUCKLING DEFORMATIONS ON THE BUCKLING OF ECCENTRICALLY STIFFENED ORTHOTROPIC CYLINDERS

by

David L. Block

Thesis submitted to the Graduate Faculty of the

Virginia Polytechnic Institute

in candidacy for the degree of

DOCTOR OF PHILOSOPHY

in

ENGINEERING MECHANICS

APPROVED:

Chairman, Dr. Daniel Frederick

Dr. Ricardo Chicurel

Dr. R. T. Davis

Professor F. J. Maher

Dr. Leon Rutland

June 1966

Blacksburg, Virginia

II. TABLE OF CONTENTS

III. LIST OF TABLES AND FIGURES

IV. INTRODUCTION

In the design of lightweight structures the growing need for precision has increased the importance of understanding the effects of stiffening elements on the buckling behavior of cylindrical shells. The importance of one of these effects, the eccentricity or one-sidness of stiffening elements, on the buckling strength has been demonstrated in several studies (see refs. 1 - 7). For geometry of a typical stiffened cylinder see figure 1. The theoretical eccentricity investigations of references 1 through 5 and the experimental investigations of references 6 and 7 have illustrated the importance of eccentricities, but it would be much more desirable if better agreement could be obtained between the experimental results and the theoretical results. These differences between experiment and theory show a need for additional considerations in the theories such as prebuckling deformations, discrete stiffeners, initial imperfections, and boundary conditions.

The purpose of the present paper is to present a theoretical investigation in which prebuckling deformations and discrete stiffener effects are included in the analysis. The effect of discrete stiffeners is studied only for rings or circumferential stiffeners because for practical sized stiffened cylinders the longitudinal stiffeners or stringers are closely spaced and therefore can be assumed to be average or "smeared out" over the stringer spacing, whereas, the rings are not necessarily closely spaced. In the present paper the only boundary conditions considered are those of classical simple support.

The importance of prebuckling deformations has been demonstrated for unstiffened isotropic cylinders (see refs. 8 and 9) and for stiffened isotropic cylinders in reference 5. In reference 5, the stiffeners are assumed smeared out and a two mode Galerkin solution is used to obtain the buckling loads. The results of reference 5 show an edge moment effect but do not directly assess the prebuckling deformations effect.

The importance of discrete rings has been studied in reference 10 for orthotropic cylinders in axial compression, but the theory used did not consider eccentricities of stiffeners or prebuckling deformations. In reference 4 a discrete ring theory is presented for stiffened isotropic cylinders but prebuckling deformations are neglected.

In view of the great variety of stiffened shell configurations that are under consideration by designers, a buckling analysis is needed which is applicable to a broad class of structures. Such an analysis is presented in the present paper by considering a cylindrical shell constructed from orthotropic material with stiffening elements on its surface. By proper definition of the orthotropic material constants such an analysis can be used to predict buckling for a wide variety of stiffened shells, for example, sandwich-type, corrugated, filament-wound or isotropic cylinders.

Nonlinear equilibrium equations and boundary conditions are derived for the eccentrically stiffened orthotropic cylinder with discrete rings. The derivation is performed by defining nonlinear strain-displacement relations for the cylinder and the stiffeners, treating the stiffeners as beam elements. The strain energy of the stiffener-cylinder system is then formulated and the nonlinear equilibrium equations and boundary conditions are obtained by applying the principle of minimum potential energy. By a perturbation of the nonlinear equilibrium equations and boundary conditions, a set of nonlinear prebuckling equations and boundary conditions and linear buckling equations and boundary conditions are obtained.

Solutions to the prebuckling and buckling equations are obtained for classical simple support boundary conditions by the method of finite differences of reference 11. The finite difference method of solution which is used employs a reduction of the governing equations to a second order system of equations, a matrix formulation of the finite difference equations, and a modified Gaussian elimination procedure of solution. Similar type solutions are presented when the rings are considered to be smeared out. In appendix A, a Galerkin solution is presented for the classical buckling problem of discrete rings in which prebuckling deformations are assumed constant.

Due to the large number of parameters involved in the problem, results of a general nature are impractical to present. However, results in the form of sample calculations are presented for two cylinders of contemporary proportions, that is, ring- and stringer-stiffened isotropic cylinders and ring-stiffened corrugated cylinders. The calculations illustrate the influence of discrete and smeared out rings, prebuckling deformations, and eccentrically applied compressive loads (applied edge moments) on the buckling loads of stiffened cylinders. Prebuckling and buckling shapes are also presented.

V. SYMBOLS

A	cross sectional area of stiffener
A_i, B_i, C_i, $\bar{A}_{o(k)}$, $\bar{B}$, $\bar{C}_{o(k)}$	4×4 matrices defined by equations (55), (66), and (59)
D_x, D_y	bending stiffness of orthotropic plate in longitudinal and circumferential directions, respectively
$\bar{D}_x$	longitudinal bending stiffness parameter, $\frac{D_x}{1-\mu_x\mu_y} + \frac{E_sI_s}{d} + \frac{E_sA_s\bar{z}_s^2}{d}$
D_{xy}	twisting stiffness of orthotropic plate
E	Young's modulus
E_x, E_y	extensional stiffness of orthotropic plate in longitudinal and circumferential directions, respectively
$\bar{E}_x$	longitudinal extensional stiffness parameter, $\frac{E_x}{1-\mu_x'\mu_y'} + \frac{E_sA_s}{d}$
$F_1 \rightarrow F_{11}$	constants defined by equation (A7)
G	shear modulus
G_{xy}	in-plane shear stiffness of orthotropic plate
I	moment of inertia of stiffener about its centroid

I_o	moment of inertia of stiffener about middle surface of shell
J	torsional constant for stiffener
L_i, S, $\overline{S}$	2×2 matrices defined by equations (41)
M_x, M_y, M_{xy}	middle surface moment resultants
$\overline{M}_x$, $\overline{M}_y$, $\overline{M}_{xy}$	bending and twisting moments in orthotropic shell
N_x, N_y, N_{xy}	middle surface stress resultants
$\overline{N}_x$, $\overline{N}_y$, $\overline{N}_{xy}$	normal and shearing forces in orthotropic shell
$\hat{N}_x$	externally applied longitudinal compressive load resultant
N	total number of rings on cylinder
P_i	4×4 recurrence relation matrices defined by equation (62) and equation (63)
$\overline{P}_i$, $\overline{Q}_i$	2×2 recurrence relation matrices defined by equation (44) and equation (46)
R	radius of cylinder to middle surface of orthotropic shell (see fig. 1)
U, V, W, M	functions of x which appear in buckling displacements u_B, v_B, w_B, and M_{xB} defined by equation (51)

Z_A	1×2 column matrix defined by equation (41)
Z_B	1×4 column matrix defined by equation (55)
a	length of stiffened cylinder (see fig. 1)
a_q, b_q, c_q	constant coefficients of equation (A4)
d	stringer spacing (see fig. 1)
$\bar{e}$	distance from middle surface of cylinder to line on which $\hat{N}_x$ acts
h	one-half the height of the stringer section (see fig. 2)
i	finite difference station indice
j, q, r, s	integers
k	total number of finite difference stations along length of cylinder
l	ring spacing (see fig. 1)
m	number of finite difference spaces (Δ) between rings
n	number of full waves in cylinder buckle pattern in circumferential direction
p	external pressure
t	thickness of isotropic cylinder shell wall (see fig. 1)

$\bar{t}$	effective wall thickness of stiffened isotropic cylinder, $\frac{A_s}{d} + t$
t_c	thickness of corrugation (see fig. 2)
u, v, w	middle surface displacements of orthotropic shell in x-, y-, and z- directions, respectively
x, y, z	orthogonal curvilinear coordinates with origin lying in middle surface of orthotropic shell (see fig. 1)
$\bar{z}$	distance from centroid of stiffener to middle surface of orthotropic shell (see fig. 1), positive if stiffener lies on external surface of shell
$\alpha_1, \alpha_2, \gamma_1, \gamma_2, \gamma_3, \gamma_4, \kappa$	constants defined by equation (50)
$\beta_1, \beta_2, \beta_3, \beta_4, \beta_5, \beta_6$	constants defined by equation (24) and equation (37)
Δ	distance between adjacent finite difference stations
Π	total potential energy of stiffened cylinder
Π_c, Π_r, Π_s	strain energy of orthotropic shell, rings, and stringers, respectively
Π_L	potential energy of external forces
$\epsilon_x, \epsilon_y, \gamma_{xy}$	normal and shearing strains at middle surface of orthotropic shell

ϵ_{xT}, ϵ_{yT}, γ_{xyT}	normal and shearing strains in orthotropic shell
ϵ_{yr}, ϵ_{xs}	strains in rings and stringers, respectively
$\Lambda_1 \rightarrow \Lambda_{24}$	constants defined by equation (53)
$\delta(x - j\,l)$	Dirac delta function defined such that $\int_{-\infty}^{+\infty} f(x)\delta(x-jl)dx = f(jl)$, where $\delta(x-jl) = 0$, when $x \neq jl$
δ_{ij}	Kronecker delta, $\delta_{ij} = 0$ when $i \neq j$ and $\delta_{ij} = 1$ when $i = j$
μ_x, μ_y	Poisson's ratios for bending of orthotropic plate in longitudinal and circumferential directions, respectively
μ_x', μ_y'	Poisson's ratios for extensions of orthotropic plate in longitudinal and circumferential directions, respectively
Φ_r, Φ_{rq}, ψ_r, ψ_{rq}	defined by equation (A9)
$\xi = w_{A,xx}$	

Subscripts:

r	refers to rings (circumferential stiffening, parallel to y-axis)

s	refers to stringers (longitudinal stiffening, parallel to x-axis)
A	refers to prebuckling state
B	refers to small changes away from prebuckling state which occur at buckling
M	value of finite difference station at which ring is located

A subscript preceded by a comma indicates partial differentiation with respect to the subscript.

VI. DERIVATION OF THEORY

To develop the buckling theory for the stiffened cylinder, shown in figure 1, several basic assumptions are made. The stiffened cylinder is composed of an orthotropic shell stiffened by uniform equally spaced rings and stringers, all having elastic properties. The elastic constants of the orthotropic shell are taken as those given in reference 12, with the assumption that the transverse shearing stiffnesses of the shell are infinitely large. The stringers are assumed to be closely spaced so that their elastic properties can be averaged over the stringer spacing. However, the rings are considered to be located along a circumferential line on the cylinder (discretely located on the shell). In cases where both rings and stringers lie on the same surface of the shell, the effect of the joints in the stiffener frame work is ignored. The eccentricities of the rings and stringers are considered. The only applied loadings considered are an axial compressive end load and a constant external pressure load.

The equations are derived by obtaining strain energy expressions for the shell, stiffeners and loadings and applying the method of minimum potential energy to obtain the nonlinear equilibrium equations and boundary conditions of the configuration. Nonlinear prebuckling and linear buckling equations are then obtained by a perturbation of the displacements associated with the equilibrium equations. The following sections detail this derivation.

Strain - Displacement Relations

For the coordinate system shown in figure 1, the Donnell type nonlinear strain displacement relationships can be written as

$$\epsilon_{x_T} = \epsilon_x - zw,_{xx}$$

$$\epsilon_{y_T} = \epsilon_y - zw,_{yy}$$

$$\gamma_{xy_T} = \gamma_{xy} - 2\ zw,_{xy} \tag{1}$$

where

$$\epsilon_x = u,_x + \frac{1}{2}\, w,_x^2$$

$$\epsilon_y = v,_y + \frac{w}{R} + \frac{1}{2}\, w,_y^2$$

$$\gamma_{xy} = u,_y + v,_x + w,_x\ w,_y \tag{2}$$

The quantities u, v, and w are the displacements of the middle surface of the orthotropic cylinder wall and a comma denotes partial differentiation with respect to the subscript.

The stiffeners are assumed to behave as beam elements, thus the stiffener strain-displacement relations can be written as

$$\epsilon_{y_r} = \epsilon_y - zw,_{yy}$$

$$\epsilon_{x_s} = \epsilon_x - zw,_{xx} \tag{3}$$

where the subscripts r and s denote rings and stringers, respectively. Equations (3) specify that the displacements are such that the strain varies linearly across the depth of the stiffener and satisfies compatibility of the displacements between the stiffener and the surface of the shell to which it is fastened.

Energy of Stiffened Cylinder

Orthotropic shell.- The strain energy of the orthotropic shell Π_c can be expressed in terms of resultant middle-surface forces and moments as

$$\Pi_c = \frac{1}{2} \int_0^{2\pi R} \int_0^a \left(\overline{N}_x \epsilon_x + \overline{N}_{xy} \gamma_{xy} + \overline{N}_y \epsilon_y - \overline{M}_x w,_{xx} + 2\overline{M}_{xy} w,_{xy} - \overline{M}_y w,_{yy}\right) dx\, dy \tag{4}$$

where

$$\overline{N}_x = \frac{E_x}{1 - \mu_x'\mu_y'} \left(\epsilon_x + \mu_y'\epsilon_y\right)$$

$$\overline{N}_y = \frac{E_y}{1 - \mu_x'\mu_y'} \left(\epsilon_y + \mu_x'\epsilon_x\right)$$

$$\overline{N}_{xy} = G_{xy}\gamma_{xy}$$

$$\overline{M}_x = - \frac{D_x}{1 - \mu_x\mu_y} \left(w,_{xx} + \mu_y w,_{yy}\right)$$

$$\overline{M}_y = - \frac{D_y}{1 - \mu_x\mu_y} \left(w,_{yy} + \mu_x w,_{xx}\right)$$

$$\bar{M}_{xy} = D_{xy} w,_{xy} \tag{5}$$

and ϵ_x, ϵ_y, and γ_{xy} are given by equations (2).

Rings.- Considering the rings to be equally spaced and discretely located along the length of the cylinder, the strain energy Π_r of N rings can be expressed as

$$\Pi_r = \frac{1}{2} \sum_{j=1}^{N} \int_0^{2\pi R} \left(\int_{A_r} E_r \epsilon_{y_r}^2 \, dA_r + G_r J_r \, w,_{xy}^2 \right)_{x=jl} dy \tag{6}$$

where dA_r is an element of the cross-sectional area of the ring A_r, $G_r J_r$ is its twisting stiffness, and l is the ring spacing.

In the energy expression, the first term is the expression for the energy associated with bending and extension of a beam and the second term is inserted as an approximation to the energy due to twisting of the ring. The approximation for energy due to twisting results from assuming that the ring twists in a fashion so that its angle of twist is equal to the angle of twist of the shell.

Substituting the ring strain-displacement relation (eqs. (3)) into equation (6) and performing the integrations over the ring area, the strain energy for N rings becomes

$$\Pi_r = \frac{1}{2} \sum_{j=1}^{N} \int_0^{2\pi R} \left(E_r A_r \epsilon_y^2 - 2E_r A_r \bar{z}_r w,_{yy} \epsilon_y + E_r I_{or} w,_{yy}^2 \right.$$

$$\left. + G_r J_r w,_{xy}^2 \right)_{x=jl} dy \tag{7}$$

where $\bar{z}_r$ is the distance from the centroid of the ring to the middle surface of the shell and I_{or} is the moment of inertia of a ring about the middle surface of the shell.

Stringers.- Assuming the stringers to be closely spaced so that their elastic properties can be averaged over the stringer spacing, the strain energy of the stringers Π_s can be taken as

$$\Pi_s = \frac{1}{2} \int_0^{2\pi R} \int_0^a \left(\frac{E_s A_s}{d} \epsilon_x^2 - \frac{2E_s A_s \bar{z}_s}{d} \epsilon_x w,_{xx} + \frac{E_s I_{os}}{d} w,_{xx}^2 \right.$$

$$\left. + \frac{G_s J_s}{d} w,_{xy}^2 \right) dxdy \tag{8}$$

where d is the stringer spacing and the subscript s is used to denote stringer properties comparable to those appearing in equation (7) for the rings.

Applied loads.- Considering applied loads of a constant external pressure p and an externally applied load resultant $\hat{N}_x$ (positive in compression), the potential energy Π_L associated with these loads is

$$\Pi_L = \int_0^{2\pi R} \int_0^a pw \, dxdy + \int_0^{2\pi R} \hat{N}_x \left(u - \bar{e}w,_x\right) \Big|_0^a dy \tag{9}$$

where $\bar{e}$ is the distance from the middle surface of the orthotropic shell to the line on which the load resultant $\hat{N}_x$ acts.

Nonlinear Equilibrium Equations and Boundary Conditions

The total potential energy of the stiffened cylinder Π is the sum of the energies given by equations (4), (7), (8), and (9) and can be written as

$$\Pi = \Pi_c + \Pi_r + \Pi_s + \Pi_L \tag{10}$$

The nonlinear equilibrium equations and boundary conditions are obtained from the principle of minimum potential energy. By the calculus of variations, the minimum potential energy requires the vanishing of the first variation $\delta\Pi$. After integration by parts and proper regrouping the first variation can be evaluated from equation (10) as

$$\delta\Pi = \int_0^{2\pi R} \int_0^a \Bigg\{ \left[-N_{x,x} - \bar{N}_{xy,y}\right] \delta u + \left[-\bar{N}_{y,y} - \bar{N}_{xy,x}\right] \delta v$$

$$+ \Bigg[-M_{x,xx} + \left(2\bar{M}_{xy} + \frac{G_s J_s}{d} w,_{xy}\right)_{,xy} - \bar{M}_{y,yy} + \left(-N_{x,x} - \bar{N}_{xy,y}\right) w,_x$$

$$+ \left(-\overline{N}_{y,y} - \overline{N}_{xy,x}\right) w,_y + \frac{\overline{N}_y}{R} - N_x w,_{xx} - \overline{N}_y w,_{yy} - 2\overline{N}_{xy} w,_{xy}$$

$$+ p\Bigg] \delta w\Bigg\} \, dxdy + \int_0^{2\pi R} \Bigg\{ \left[N_x + \hat{N}_x\right] \delta u + \overline{N}_{xy} \, \delta v$$

$$+ \left[-M_x - \hat{N}_x \overline{e}\right] \delta w,_x + \Bigg[M_{x,x} + N_x w,_x + \overline{N}_{xy} w,_y$$

$$- \left(2\overline{M}_{xy} + \frac{G_s J_s}{d}\right)_{,y}\Bigg] \delta w\Bigg\}\Bigg|_0^a dy + \int_0^{2\pi R} \sum_{j=1}^{N} \Bigg\{\Bigg[-E_r A_r \Big(\epsilon_y$$

$$- \overline{z}_r w,_{yy}\Big)_{,y}\Bigg] \delta v - \left[G_r J_r w,_{xyy}\right] \delta w,_x + \Bigg[\Big(E_r A_r \overline{z}_r \epsilon_y$$

$$- E_r I_{or} w,_{yy}\Big)_{,yy} + \frac{E_r A_r}{R} \left(\epsilon_y - \overline{z}_r w,_{yy}\right) - E_r A_r w,_y \left(\epsilon_y - \overline{z}_r w,_{yy}\right)_{,y}$$

$$- E_r A_r \left(\epsilon_y - \overline{z}_r w,_{yy}\right) w,_{yy}\Bigg] \delta w\Bigg\}_{x=jl} dy = 0 \qquad (11)$$

where

$$N_x = \frac{E_x}{1 - \mu_x' \mu_y'} \left[u,_x + \frac{1}{2} w,_x^2 + \mu_y' \left(v,_y + \frac{w}{R} + \frac{1}{2} w,_y^2\right)\right]$$

$$+ \frac{E_s A_s}{d} \left(u,_x + \frac{1}{2} w,_x^2 - \overline{z}_s w,_{xx}\right)$$

$$M_x = - \Bigg[\frac{D_x}{1 - \mu_x \mu_y} \left(w,_{xx} + \mu_y w,_{yy}\right) + \frac{E_s I_{os}}{d} w,_{xx}$$

$$- \frac{E_s A_s \overline{z}_s}{d} \left(u,_x + \frac{1}{2} w,_x^2\right)\Bigg] \qquad (12)$$

and $\overline{N}_y$, $\overline{N}_{xy}$, $\overline{M}_y$, and $\overline{M}_{xy}$ are as given by equation (5).

Requiring equation (11) to vanish will give equilibrium equations for a stringer stiffened orthotropic cylinder with boundary conditions at each ring location and at the ends of the cylinder. For the problem considered herein, that of discrete rings, it is advantageous to have the number of rings present on the cylinder to be arbitrary. Therefore, for facility of solution, the ring terms which appear in equation (11) as boundary conditions are included in the equilibrium equations as discrete quantities by use of a Dirac delta function as follows

$$\sum_{j=1}^{N} \int_0^{2\pi R} \Big(\text{Ring terms}\Big)_{x=jl} dy = \sum_{j=1}^{N} \int_0^{2\pi R} \int_0^{a} \Big(\text{Ring terms}\Big) \delta\left(x-jl\right) dx dy \tag{13}$$

where the Dirac delta function is defined as

$$\begin{aligned} \int_{-\infty}^{+\infty} f(x)\ \delta(x - jl)\ dx &= f(jl) \quad \text{when} \quad x = jl \\ &= 0 \quad\quad \text{when} \quad x \neq jl \end{aligned}$$

By use of equation (13), the first variation of the energy can now be written in terms of stress and moment resultants as

$$\delta\Pi = \int_0^{2\pi R} \int_0^{a} \Bigg\{ \Big[-N_{x,x} - N_{xy,y} \Big] \delta u + \Big[-N_{y,y} - N_{xy,x} \Big] \delta v$$

$$+ \Big[-M_{x,xx} + M_{xy,xy} - M_{y,yy} + \frac{N_y}{R} - \Big(N_{x,x} + N_{xy,y} \Big) w_{,x}$$

$$-\left(N_{y,y} + N_{xy,x}\right)w,_{y} - N_{x}w,_{xx} - N_{y}w,_{yy} - 2N_{xy}w,_{xy} + p\Big]\,\delta w\Big\}\,dxdy$$

$$+ \int_0^{2\pi R}\Big\{\left(N_x + \hat{N}_x\right)\delta u + N_{xy}\,\delta v + \left(-M_x - \hat{N}_x\bar{e}\right)\delta w,_{x}$$

$$+ \left(M_{x,x} - M_{xy,y} + N_x w,_{x} + N_{xy}w,_{y}\right)\delta w\Big\}\Big|_0^a\,dy = 0 \qquad (14)$$

where

$$N_y = \frac{E_y}{1 - \mu_x'\mu_y'}\left[v,_{y} + \frac{w}{R} + \frac{1}{2}\,w,_{y}^{2} + \mu_x'\,\left(u,_{x} + \frac{1}{2}\,w,_{x}^{2}\right)\right]$$

$$+ \sum_{j=1}^{N}\delta(x - jl)\;E_rA_r\left(v,_{y} + \frac{w}{R} + \frac{1}{2}\,w,_{y}^{2} - \bar{z}_r\,w,_{yy}\right)$$

$$N_{xy} = G_{xy}\,\left(u,_{y} + v,_{x} + w,_{x}w,_{y}\right)$$

$$M_y = -\Bigg\{\frac{D_y}{1 - \mu_x\mu_y}\,\left(w,_{yy} + \mu_x w,_{xx}\right) + \sum_{j=1}^{N}\delta(x - jl)\Big[E_rI_{or}\,w,_{yy}$$

$$- E_rA_r\bar{z}_r\,\left(v,_{y} + \frac{w}{R} + \frac{1}{2}\,w,_{y}^{2}\right)\Big]\Bigg\}$$

$$M_{xy} = \left(2D_{xy} + \frac{G_sJ_s}{d} + \sum_{j=1}^{N}\delta(x - jl)\;G_rJ_r\right)w,_{xy} \qquad (15)$$

and N_x and M_x are defined by equations (12).

The nonlinear equilibrium equations which govern an eccentrically stiffened orthotropic cylinder with discrete rings are now

$$N_{x,x} + N_{xy,y} = 0$$

$$N_{y,y} + N_{xy,x} = 0$$

$$-M_{x,xx} + M_{xy,xy} - M_{y,yy} + \frac{N_y}{R} - N_x w,_{xx} - N_y w,_{yy} - 2N_{xy} w,_{xy} + p = 0 \tag{16}$$

with boundary conditions to be satisfied at each end of the cylinder of

$$N_x + \hat{N}_x = 0 \qquad \text{or} \qquad u = 0$$

$$N_{xy} = 0 \qquad \text{or} \qquad v = 0$$

$$M_x + \hat{N}_x \bar{e} = 0 \qquad \text{or} \qquad w,_x = 0$$

$$M_{x,x} - M_{xy,y} + N_x w,_x + N_{xy} w,_y = 0 \quad \text{or} \qquad w = 0 \tag{17}$$

where the stress and moment resultants in equations (16) and (17) are given by equations (12) and (15).

Prebuckling and Buckling Equations

In this section, the nonlinear equilibrium equations and boundary conditions (eqs. (16) and (17)) are used to obtain the equations and boundary conditions which govern the prebuckling and buckling of a stiffened cylinder with discrete rings. To obtain the prebuckling and buckling equations, the displacements of the shell u, v, and w are assumed separable into two parts as follows

$$u(x,y) = u_A(x) + u_B(x,y)$$

$$v(x,y) = v_A(x) + v_B(x,y)$$

$$w(x,y) = w_A(x) + w_B(x,y) \tag{18}$$

The first part, denoted by the subscript A, is an axisymmetric prebuckling displacement. The second part, denoted by B, is the infinitesimal nonaxisymmetric displacement that occurs at buckling.

The equilibrium equations which govern the axisymmetric prebuckling are obtained from substitution of the axisymmetric displacement in equations (18) into equations (16) and are found to be

$$N_{x_{A,x}} = 0$$

$$N_{xy_{A,x}} = 0$$

$$-M_{x_{A,xx}} + \frac{N_{y_A}}{R} - N_{x_A} w_{A,xx} + p = 0 \tag{19}$$

The appropriate set of boundary conditions are found similarly from equations (17) to be

$$N_{x_A} + \hat{N}_x = 0 \qquad \text{or} \qquad u_A = 0$$

$$N_{xy_A} = 0 \qquad \text{or} \qquad v_A = 0$$

$$M_{x_A} + \hat{N}_x \bar{e} = 0 \qquad \text{or} \qquad w_{A,x} = 0$$

$$M_{x_{A,x}} + N_{x_A} w_{A,x} = 0 \qquad \text{or} \qquad w_A = 0 \qquad (20)$$

where in equations (19) and (20)

$$N_{x_A} = \frac{E_x}{1 - \mu_x'\mu_y'}\left(u_{A,x} + \frac{1}{2} w_{A,x}^{\;2} + \mu_y' \frac{w_A}{R}\right) + \frac{E_s A_s}{d}\left(u_{A,x} + \frac{1}{2} w_{A,x}^{\;2} - \bar{z}_s w_{A,xx}\right)$$

$$N_{y_A} = \frac{E_y}{1 - \mu_x'\mu_y'}\left[\frac{w_A}{R} + \mu_x'\left(u_{A,x} + \frac{1}{2} w_{A,x}^{\;2}\right)\right] + \sum_{j=1}^{N} \delta(x - jl)\, E_r A_r \frac{w_A}{R}$$

$$N_{xy_A} = G_{xy} v_{A,x}$$

$$M_{x_A} = -\left[\left(\frac{D_x}{1 - \mu_x\mu_y} + \frac{E_s I_{os}}{d}\right) w_{A,xx} - \frac{E_s A_s \bar{z}_s}{d}\left(u_{A,x} + \frac{1}{2} w_{A,x}^{\;2}\right)\right] \qquad (21)$$

The first of equations (19) and (20) requires that N_{xA} = constant = $-\hat{N}_x$. The second of equations (19) and (20) requires that N_{xyA} = constant = 0 (no applied shear). From the first two equations of equations (21) together with $N_{xA} = -\hat{N}_x$, N_{yA} can be written as

$$N_{yA} = \frac{E_y \mu_x' E_s A_s \bar{z}_s}{\bar{E}_x\left(1 - \mu_x'\mu_y'\right)d} w_{A,xx} + \left[\frac{E_y\left(E_x + \frac{E_s A_s}{d}\right)}{\bar{E}_x R\left(1 - \mu_x'\mu_y'\right)} + \sum_{j=1}^{N} \delta(x - jl) \frac{E_r A_r}{R}\right] w_A - \frac{E_y \mu_x'}{\bar{E}_x\left(1 - \mu_x'\mu_y'\right)} \hat{N}_x \qquad (22)$$

where

$$\bar{E}_x = \frac{E_x}{1 - \mu_x'\mu_y'} + \frac{E_s A_s}{d}$$

The equation determining the prebuckling deflection is now obtained from equations (19), (21), and (22) as

$$\beta_1 w_{A,xxxx} + \beta_2 w_{A,xx} + \left[\beta_3 + \sum_{j=1}^{N} \delta(x - jl)\, \beta_4\right] w_A - \beta_5 = 0 \qquad (23)$$

where

$$\beta_1 = \frac{D_x}{1 - \mu_x\mu_y} + \frac{E_s I_s}{d} + \frac{E_s A_s \bar{z}_s^2 E_x}{\bar{E}_x\left(1 - \mu_x'\mu_y'\right)d}$$

$$\beta_2 = \frac{2E_y \mu_x' E_s A_s \bar{z}_s}{\bar{E}_x R\left(1 - \mu_x'\mu_y'\right)d} + \hat{N}_x$$

$$\beta_3 = \frac{E_y}{\bar{E}_x R^2\left(1 - \mu_x'\mu_y'\right)} \left(E_x + \frac{E_s A_s}{d}\right)$$

$$\beta_4 = \frac{E_r A_r}{R^2}$$

$$\beta_5 = \frac{E_y \mu_x'}{\bar{E}_x R\left(1 - \mu_x'\mu_y'\right)} \hat{N}_x - p \tag{24}$$

and $I_s = I_{os} - A_s \bar{z}_s^2$ with boundary conditions to be satisfied of:

$$M_{x_A} + \hat{N}_x \bar{e} = 0 \qquad \text{or} \qquad w_{A,x} = 0$$

$$M_{x_{A,x}} - \hat{N}_x w_{A,x} = 0 \qquad \text{or} \qquad w_A = 0 \tag{25}$$

The equilibrium equations and boundary conditions which govern the buckling of a stiffened cylinder with discrete rings are obtained by substituting equations (18) into equations (16) and (17). If only linear terms in the buckling displacements (subscript B terms) are retained, and if identities (19) are subtracted out, the following buckling equations are obtained

$$N_{x_{B,x}} + N_{xy_{B,y}} = 0$$

$$N_{y_{B,y}} + N_{xy_{B,x}} = 0$$

$$-M_{x_{B,xx}} + M_{xy_{B,xy}} - M_{y_{B,yy}} + \frac{N_{y_B}}{R} - N_{x_A} w_{B,xx} - N_{x_B} w_{A,xx}$$

$$- N_{y_A} w_{B,yy} - 2N_{xy_A} w_{B,xy} = 0 \qquad (26)$$

with the boundary conditions of

$$N_{x_B} = 0 \qquad \text{or} \qquad u_B = 0$$

$$N_{xy_B} = 0 \qquad \text{or} \qquad v_B = 0$$

$$M_{x_B} = 0 \qquad \text{or} \qquad w_{B,x} = 0$$

$$M_{x_{B,x}} - M_{xy_{B,y}} + N_{x_A} w_{B,x} + N_{x_B} w_{A,x} + N_{xy_A} w_{B,y} = 0$$

or

$$w_B = 0 \qquad (27)$$

where

$$N_{x_B} = \frac{E_x}{1 - \mu_x' \mu_y'} \left[u_{B,x} + w_{A,x} w_{B,x} + \mu_y' \left(v_{B,y} + \frac{w_B}{R} \right) \right]$$

$$+ \frac{E_s A_s}{d} \left(u_{B,x} + w_{A,x} w_{B,x} - \bar{z}_s \, w_{B,xx} \right)$$

$$N_{y_B} = \frac{E_y}{1 - \mu_x'\mu_y'}\left[v_{B,y} + \frac{w_B}{R} + \mu_x'\left(u_{B,x} + w_{A,x}w_{B,x}\right)\right]$$

$$+ \sum_{j=1}^{N} \delta(x - jl)\, E_r A_r \left(v_{B,y} + \frac{w_B}{R} - \bar{z}_r\, w_{B,yy}\right)$$

$$N_{xy_B} = G_{xy}\left(u_{B,y} + v_{B,x} + w_{A,x}w_{B,y}\right)$$

$$M_{x_B} = -\left[\frac{D_x}{1 - \mu_x\mu_y}\left(w_{B,xx} + \mu_y\, w_{B,yy}\right) + \frac{E_s I_s}{d}\, w_{B,xx}\right.$$

$$\left. - \frac{E_s A_s \bar{z}_s}{d}\left(u_{B,x} + w_{A,x}w_{B,x} - \bar{z}_s\, w_{B,xx}\right)\right]$$

$$M_{y_B} = -\left\{\frac{D_y}{1 - \mu_x\mu_y}\left(w_{B,yy} + \mu_x\, w_{B,xx}\right) + \sum_{j=1}^{N} \delta(x - jl)\left[E_r I_r w_{B,yy}\right.\right.$$

$$\left.\left. - E_r A_r \bar{z}_r\left(v_{B,y} + \frac{w_B}{R} - \bar{z}_r\, w_{B,yy}\right)\right]\right\}$$

$$M_{xy_B} = \left[2D_{xy} + \frac{G_s J_s}{d} + \sum_{j=1}^{N} \delta(x - jl)\, G_r J_r\right] w_{B,xy}$$

and

$$I_r = I_{or} - A_r\, \bar{z}_r^2 \tag{28}$$

To solve the buckling equations (26) and boundary conditions (27), the prebuckling quantities (subscript A) must first be determined by solution of the prebuckling equation (23) and boundary conditions (25). The solution of the prebuckling and buckling equations is discussed in the next section.

VII. SOLUTIONS

In this section solutions of the prebuckling and buckling equations are obtained by use of the finite difference method. The prebuckling and buckling equations are solved employing a technique suggested by Budiansky and Radkowski in reference 11 in which the system of governing differential equations is changed to a system of second order differential equations and then these equations are written in terms of finite differences. The resulting difference equations are then written in matrix form and solved by a modified Gaussian elimination technique. In all cases, the solutions are for classical simple support boundary conditions. Details of the solutions follow.

Solution of Prebuckling Equation

The governing equation for the prebuckling displacement, equation (23) developed in the previous section, is a fourth order variable coefficient ordinary differential equation and in order to employ the technique of solution of reference 11 it must be changed to a system of second order differential equations. This change is accomplished by letting

$$\xi = w_{A,xx} \tag{29}$$

then equation (23) can be written as

$$\beta_1 \xi,_{xx} + \beta_2 \xi + \left[\beta_3 + \sum_{j=1}^{N} \delta(x-jl)\beta_4\right] w_A - \beta_5 = 0 \tag{30}$$

where β_1 through β_5 are as defined by equations (24). Equations (29) and (30) are now the governing equations for the prebuckling displacements.

When the derivatives occuring in equations (29) and (30) are replaced by finite differences, a set of simultaneous linear algebraic equations for the values of w_A and ξ at discrete points along the length of the cylinder are obtained. The stations along the length of the cylinder are taken to be equally spaced and are numbered from $i = 0$ at the end of the cylinder at $x = 0$ to $i = k$ at the end of the cylinder at $x = a$. There are also stations corresponding to $i = -1$ and $i = k + 1$. The following central difference approximations for the first and second derivatives are used

$$\left(f,_x\right)_i = \frac{f_{i+1} - f_{i-1}}{2\Delta}$$

$$\left(f,_{xx}\right)_i = \frac{f_{i+1} - 2f_i + f_{i-1}}{\Delta^2} \tag{31}$$

where i indicates the station and Δ is the distance between adjacent stations. When equations (31) are substituted, equations (29) and (30) for $i = 1, 2, \ldots., k -1$ become

$$\beta_1\left(\frac{\xi_{i+1} - 2\xi_i + \xi_{i-1}}{\Delta^2}\right) + \beta_2\xi_i + \left(\beta_3 + \frac{\delta_{1M}\beta_4}{\Delta}\right)w_{A_i} - \beta_5 = 0$$

$$\frac{w_{A_{i+1}} - 2w_{A_i} + w_{A_{i-1}}}{\Delta^2} - \xi_i = 0 \tag{32}$$

where

$$\delta_{iM} = 1 \qquad \text{if} \qquad i = M$$

$$\delta_{iM} = 0 \qquad \text{if} \qquad i \neq M$$

The value of the subscript M is the value of the difference station at which a ring is located and can be expressed as

$$M = mj \qquad (j = 1,2,\ldots N) \qquad (33)$$

where m is the number of difference spaces (Δ) between adjacent rings and N is the total number of rings on the cylinder as previously defined. In the finite difference equations (32), the ring properties are assumed to be applicable (smeared out or averaged) over one difference spacing (Δ). At each of the stations ξ_i and w_{A_i} are unknowns, hence the total number of unknowns is $2(k+1)$. Equations (32) represent $2(k-1)$ equations. The boundary conditions yield the needed four additional equations thus giving $2(k+1)$ equations and $2(k+1)$ unknowns.

From equations (25) the boundary conditions for simple supports at $x = 0$ and $x = a$ are

$$M_{x_A} = - \hat{N}_x \overline{e}$$

$$w_A = 0 \qquad (34)$$

Using equations (21) and (31), the boundary conditions in terms of finite differences can be written as follows:

At station $i = o$ $(x=o)$

$$\xi_o = \frac{\beta_6}{\beta_1}$$

$$w_{A_o} = o \qquad (35)$$

At station $i = k$ $(x=a)$

$$\xi_k = \frac{\beta_6}{\beta_1}$$

$$w_{A_k} = 0 \tag{36}$$

where

$$\beta_6 = \hat{N}_x \left(\bar{e} - \frac{E_s A_s \bar{z}_s}{\bar{E}_x d} \right) \tag{37}$$

and β_1 is as defined by equations (24).

The governing difference equations (32) and boundary conditions (35) and (36) will now be solved by a matrix solution. Equations (32) can be written in matrix form as

$$Z_{A_{i-1}} + L_i Z_{A_i} + Z_{A_{i+1}} = S$$

$$i = 1,2,\ldots k-1 \tag{38}$$

and equations (35) and (36) as

$$Z_{A_o} = \bar{S} \tag{39}$$

$$Z_{A_k} = \bar{S} \tag{40}$$

where

$$Z_{A_i} = \begin{bmatrix} \xi_i \\ w_{A_i} \end{bmatrix}$$

$$L_i = \begin{bmatrix} \left(-2 + \dfrac{\Delta^2 \beta_2}{\beta_1}\right) & \left(\dfrac{\Delta^2 \beta_3}{\beta_1} + \dfrac{\Delta\ \beta_4 \delta_{iM}}{\beta_1}\right) \\ -\Delta^2 & -2 \end{bmatrix}$$

$$S = \begin{bmatrix} \dfrac{\Delta^2 \beta_5}{\beta_1} \\ \\ 0 \end{bmatrix}$$

$$\bar{S} = \begin{bmatrix} \dfrac{\beta_6}{\beta_1} \\ \\ 0 \end{bmatrix} \tag{41}$$

The set of matrix equations (38), (39), and (40) are solved by the method of reference 11 which is equivalent to a Gaussian elimination. This method proceeds as follows: the first of equations (38) together with equation (39) is solved for Z_{A_1} in terms of Z_{A_2}; this result is substituted into the next of equations (38) and Z_{A_2} is found in terms of Z_{A_3} and so on; finally the last of equations (38) together with equation (40) determines $Z_{A_{k-1}}$ in terms $Z_{A_{k-1}}$ and then all of the Z_A's are calculated in reverse order. Using the procedure just described, it follows from the first of equations (38) and equation (39) that

$$Z_{A_1} = L_1^{-1} \left[- Z_{A_2} + S - \bar{S} \right] \tag{42}$$

Now the general result for Z_{A_i} can be written in terms of $Z_{A_{i+1}}$ as

$$Z_{A_i} = \bar{P}_i \, Z_{A_{i+1}} + \bar{Q}_i \tag{43}$$

From equation (42) and equation (43) for $i = 1$, $\bar{P}_1$ and $\bar{Q}_1$ can be determined as

$$\bar{P}_1 = - L_1^{-1}$$

$$\overline{Q}_1 = L_1^{-1} \left[S - \overline{S} \right] \tag{44}$$

The substitution of $Z_{A_{i-1}} = \overline{P}_{i-1} Z_{A_i} + \overline{Q}_{i-1}$ into the general equation (38) gives

$$Z_{A_i} = \left[\overline{P}_{i-1} + L_i \right]^{-1} \left[- Z_{A_{i+1}} + S - \overline{Q}_{i-1} \right] \tag{45}$$

$$i = 2,3,\ldots k-1$$

Comparing equation (45) with (43) gives

$$\overline{P}_i = - \left[\overline{P}_{i-1} + L_i \right]^{-1}$$

$$\overline{Q}_i = \left[\overline{P}_{i-1} + L_i \right]^{-1} \left[S - Q_{i-1} \right] \tag{46}$$

$$i = 2,3,\ldots k-1$$

where the initial value of $\overline{P}$ and $\overline{Q}$ is given by equation (44). The recurrence relation equations (46) provide all the $\overline{P}$'s and $\overline{Q}$'s up to $\overline{P}_{k-1}$ and $\overline{Q}_{k-1}$. Equation (40) provides the value of Z_{A_k} and thus $Z_{A_{k-1}}$ is determined from equation (43) as

$$Z_{A_{k-1}} = \overline{P}_{k-1} \overline{S} + \overline{Q}_{k-1} \tag{47}$$

Now $Z_{A_{k-2}}$, $Z_{A_{k-3}}$, ... , Z_{A_1} can be determined from equation (43). For this solution the only matrix inversions for the Z_A's are of 2×2 matrices, therefore, the solution is well adapted for high speed computer computation. Once the Z_A's have been calculated, the prebuckling displacements w_A at any station along the cylinder are known.

Solution of Prebuckling Equation for Smeared Rings

It is of interest to present the solution of the prebuckling equation for the case where the rings are assumed to be smeared out over the ring spacing in order to compare with the discrete ring case. When the rings are smeared out, the prebuckling governing equation (23) becomes the following constant coefficient differential equation

$$\beta_1 w_{A,xxxx} + \beta_2 w_{A,xx} + \left[\beta_3 + \frac{\beta_4}{l}\right] w_A - \beta_5 = 0 \tag{48}$$

where l is the ring spacing and β_1 through β_5 are as previously defined by equation (24). Equation (48) has an analytical solution that satisfied boundary conditions (34) of

$$w_A = \gamma_1 \sin \alpha_1 x \sinh \alpha_2 x + \gamma_2 \sin \alpha_1 x \cosh \alpha_2 x + \gamma_3 \cos \alpha_1 x \cosh \alpha_2 x + \gamma_4 \cos \alpha_1 x \sinh \alpha_2 x + \frac{\beta_5}{\left(\beta_3 + \frac{\beta_4}{l}\right)} \tag{49}$$

where

$$\alpha_1 = \sqrt{\frac{\kappa^2}{2} + \frac{\beta_2}{4\beta_1}}$$

$$\alpha_2 = \sqrt{\frac{\kappa^2}{2} - \frac{\beta_2}{4\beta_1}}$$

$$\kappa^2 = \sqrt{\frac{\beta_3 + \frac{\beta_4}{l}}{\beta_1}}$$

$$\gamma_1 = \frac{\left(\alpha_2^2 - \alpha_1^2\right) \beta_5}{2\alpha_1\alpha_2 \left(\beta_3 + \frac{\beta_4}{l}\right)} + \frac{\beta_6}{2\alpha_1\alpha_2\beta_1}$$

$$\gamma_2 = \frac{\left(\cos \alpha_1 a - \cosh \alpha_2 a\right)\left\{\sinh \alpha_2 a \left[\frac{\beta_6}{\beta_1} + \frac{\beta_5\left(\alpha_2^2-\alpha_1^2\right)}{\left(\beta_3 + \frac{\beta_4}{l}\right)}\right] + \frac{2\alpha_1\alpha_2\ \beta_5 \sin \alpha_1 a}{\left(\beta_3 + \frac{\beta_4}{l}\right)}\right\}}{2\alpha_1\alpha_2\left[\left(\cos \alpha_1 a \sinh \alpha_2 a\right)^2 + \left(\sin \alpha_1 a \cosh \alpha_2 a\right)^2\right]}$$

$$\gamma_3 = -\frac{\beta_5}{\left(\beta_3 + \frac{\beta_4}{l}\right)}$$

$$\gamma_4 = \frac{\left(\cos \alpha_1 a - \cosh \alpha_2 a\right)\left\{\sin \alpha_1 a \left[\frac{\beta_6}{\beta_1} + \frac{\beta_5\left(\alpha_2^2-\alpha_1^2\right)}{\left(\beta_3 + \frac{\beta_4}{l}\right)}\right] - \frac{2\alpha_1\alpha_2\ \beta_5 \sinh \alpha_2 a}{\left(\beta_3 + \frac{\beta_4}{l}\right)}\right\}}{2\alpha_1\alpha_2\left[\left(\cos \alpha_1 a \sinh \alpha_2 a\right)^2 + \left(\sin \alpha_1 a \cosh \alpha_2 a\right)^2\right]} \qquad (50)$$

and β_6 is defined by equation (37). Similar type solutions for prebuckling displacements are reported in references 5, 8 and 9.

Solution of Buckling Equations

The buckling load of a stiffened orthotropic cylinder with discrete rings can be obtained by solving the previously developed buckling equations (26) along with the appropriate boundary conditions (27). In equations (26) and (27), the conditions of continuity around the cylinder are satisfied if

$$u_B = U(x) \cos \frac{ny}{R}$$

$$v_B = V(x) \sin \frac{ny}{R}$$

$$w_B = W(x) \cos \frac{ny}{R}$$

$$M_{x_B} = M(x) \cos \frac{ny}{R} \tag{51}$$

where n, the number of circumferential waves, is an integer. The buckling equations (26) may now be converted to ordinary differential equations with variable coefficients. The last of equations (51) is introduced to change the conventional eighth order system of three equations in U, V, and W to a system of four second order equations in U, V, W, and M. By making this change the finite difference method of solution previously described for the prebuckling equation can be employed. In buckling equations (26), one additional step has to be performed in order to prevent the appearance of derivatives of x of higher order than two. A higher order derivative in w_B will appear when the N_{xB} term is differentiated in the first of equations (26). From equations (28) this higher order derivative is eliminated as follows: the M_{xB} equation is solved for $w_{B,xx}$; this result is substituted into the N_{xB} equation thus giving N_{xB} in terms of M_{xB} and derivatives of x of less than second order. In performing this step and in substituting equations (51) and equation (22) for N_{yA}, the following variable coefficient second order ordinary differential equations for the buckling load are obtained

$$\Lambda_1 U,_{xx} - \Lambda_2 U + \Lambda_3 V,_x + \Lambda_1 w_{A,x} W,_{xx} + \left(\Lambda_1 w_{A,xx} + \Lambda_4\right) W,_x$$

$$- \Lambda_2 w_{A,x} W + \Lambda_5 M,_x = 0$$

$$- \Lambda_3 U,_x + \Lambda_6 V,_{xx} - \left[\Lambda_7 + \sum_{j=1}^{N} \delta(x-jl)\, \Lambda_8\right] V - \Lambda_3 w_{A,x} W,_x$$

$$- \left[\Lambda_9 + \Lambda_{10}\, w_{A,xx} + \sum_{j=1}^{N} \delta(x - j l)\, \Lambda_{11} \right] W = 0$$

$$\left(\Lambda_{12} - \Lambda_{13}\, w_{A,xx}\right) U,_x + \left[\Lambda_9 - \Lambda_{14}\, w_{A,xx} + \sum_{j=1}^{N} \delta(x - j l)\, \Lambda_{11} \right] V$$

$$+ \left[- \Lambda_{15} + \hat{N}_x + \Lambda_{16}\, w_{A,xx} - \sum_{j=1}^{N} \delta(x - j l)\, \Lambda_{17} \right] W,_{xx}$$

$$+ \left[\Lambda_{12}\, w_{A,x} - \Lambda_{13}\, w_{A,xx}\, w_{A,x} - \sum_{j=1}^{N} \delta(x - j l),_x\, \Lambda_{17} \right] W,_x$$

$$+ \left[\Lambda_{18} - \Lambda_{19}\, \hat{N}_x + \Lambda_{20}\, w_{A,xx} + \Lambda_{21}\, w_A + \sum_{j=1}^{N} \delta(x - j l) \left(\Lambda_{22} + \Lambda_{23}\, w_A\right) \right] W$$

$$- M,_{xx} = 0$$

$$- \Lambda_{16}\, U,_x + \bar{D}_x\, W,_{xx} - \Lambda_{16}\, w_{A,x}\, W,_x - \Lambda_{24}\, W + M = 0 \qquad (52)$$

where

$$\bar{D}_x = \frac{D_x}{1 - \mu_x \mu_y} + \frac{E_s I_s}{d} + \frac{E_s A_s \bar{z}_s^{\,2}}{d}$$

$$\Lambda_1 = \frac{E_x}{1 - \mu_x' \mu_y'} + \frac{E_s A_s}{\bar{D}_x\, d} \left(\frac{D_x}{1 - \mu_x \mu_y} + \frac{E_s I_s}{d} \right)$$

$$\Lambda_2 = G_{xy} \left(\frac{n}{R} \right)^2$$

$$\Lambda_3 = \left(\frac{E_x\, \mu_y'}{1 - \mu_x' \mu_y'} + G_{xy} \right) \left(\frac{n}{R} \right)$$

$$\Lambda_4 = \frac{E_x \mu'_y}{R\left(1 - \mu'_x \mu'_y\right)} - \frac{D_x \mu_y E_s A_s \bar{z}_s}{\bar{D}_x\left(1 - \mu_x \mu_y\right) d} \left(\frac{n}{R}\right)^2$$

$$\Lambda_5 = \frac{E_s A_s \bar{z}_s}{\bar{D}_x \, d}$$

$$\Lambda_6 = G_{xy}$$

$$\Lambda_7 = \frac{E_y}{\left(1 - \mu'_x \mu'_y\right)} \left(\frac{n}{R}\right)^2$$

$$\Lambda_8 = E_r \, A_r \left(\frac{n}{R}\right)^2$$

$$\Lambda_9 = \frac{E_y \, n}{R^2 \left(1 - \mu'_x \mu'_y\right)}$$

$$\Lambda_{10} = G_{xy} \left(\frac{n}{R}\right)$$

$$\Lambda_{11} = \frac{E_r \, A_r \, n}{R} \left[\frac{1}{R} + \bar{z}_r \left(\frac{n}{R}\right)^2\right]$$

$$\Lambda_{12} = \frac{E_y \, \mu'_x}{R \left(1 - \mu'_x \mu'_y\right)}$$

$$\Lambda_{13} = \frac{E_x}{1 - \mu'_x \mu'_y} + \frac{E_s \, A_s}{d}$$

$$\Lambda_{14} = \frac{E_x \mu'_y}{1 - \mu'_x \mu'_y} \left(\frac{n}{R}\right)$$

$$\Lambda_{15} = \left(\frac{D_y \mu_x}{1 - \mu_x \mu_y} + 2D_{xy} + \frac{G_s J_s}{d}\right) \left(\frac{n}{R}\right)^2$$

$$\Lambda_{16} = \frac{E_s A_s \bar{z}_s}{d}$$

$$\Lambda_{17} = G_r J_r \left(\frac{n}{R}\right)^2$$

$$\Lambda_{18} = \frac{D_y}{1 - \mu_x \mu_y} \left(\frac{n}{R}\right)^4 + \frac{E_y}{R^2\left(1 - \mu'_x \mu'_y\right)}$$

$$\Lambda_{19} = \frac{E_y \mu'_x}{\bar{\bar{E}}_x \left(1 - \mu'_x \mu'_y\right)} \left(\frac{n}{R}\right)^2$$

$$\Lambda_{20} = \frac{E_y \mu'_x E_s A_s \bar{z}_s}{\bar{\bar{E}}_x\left(1 - \mu'_x \mu'_y\right) d} \left(\frac{n}{R}\right)^2 - \frac{E_y \mu'_x}{R\left(1 - \mu'_x \mu'_y\right)}$$

$$\Lambda_{21} = \frac{E_y \left(E_x + \dfrac{E_s A_s}{d}\right)}{\bar{\bar{E}}_x R \left(1 - \mu'_x \mu'_y\right)} \left(\frac{n}{R}\right)^2$$

$$\Lambda_{22} = \left(E_r I_r + E_r A_r \bar{z}_r^2\right) \left(\frac{n}{R}\right)^4 + \frac{2 E_r A_r \bar{z}_r n^2}{R^3} + \frac{E_r A_r}{R^2}$$

$$\Lambda_{23} = \frac{E_r A_r n^2}{R^3}$$

$$\Lambda_{24} = \frac{D_x \mu_y}{\left(1 - \mu_x \mu_y\right)} \left(\frac{n}{R}\right)^2 \qquad (53)$$

and where the reciprocal relations $\mu'_x E_y = \mu'_y E_x$ and $\mu_x D_y = \mu_y D_x$ have been employed.

Writing equations (52) in finite differences at each station along the length of the cylinder, using the same numbering system as in the prebuckling solution and difference equations (31), and then writing the resulting difference equations in matrix form, the following matrix equation for $i = 0, 1, 2, \ldots k$ results

$$A_i Z_{B_{i-1}} + B_i Z_{B_i} + C_i Z_{B_{i+1}} = 0 \qquad (54)$$

where

$$Z_{B_i} = \begin{bmatrix} U_i \\ V_i \\ W_i \\ M_i \end{bmatrix}$$

$$
A_i = \begin{bmatrix}
\Lambda_1 & -\frac{\Delta\Lambda_3}{2} & \left(w_{A,x} - \frac{\Delta}{2} w_{A,xx}\right)\Lambda_1 - \frac{\Delta\Lambda_4}{2} & -\frac{\Delta\Lambda_5}{2} \\
\frac{\Delta\Lambda_3}{2} & \Lambda_6 & \frac{\Delta\Lambda_3 \, w_{A,x}}{2} & 0 \\
\frac{\Delta}{2}\left(\Lambda_{13} w_{A,xx} - \Lambda_{12}\right) & 0 & \begin{array}{l} -\Lambda_{15} + \hat{N}_x + \Lambda_{16} w_{A,xx} \\ + \frac{\Delta}{2}\left(\Lambda_{13} w_{A,xx} - \Lambda_{12}\right) w_{A,x} \\ + \frac{\Lambda_{17}}{\Delta}\left(-\frac{\delta_{(i+1)M}}{4} - \delta_{iM} - \frac{\delta_{(i-1)M}}{4}\right) \end{array} & -1 \\
\frac{\Delta\Lambda_{16}}{2} & 0 & \bar{D}_x + \frac{\Delta\Lambda_{16}}{2} w_{A,x} & 0
\end{bmatrix}
$$

$$
B_i = \begin{bmatrix}
-2\Lambda_1 - \Delta^2\Lambda_2 & 0 & -\left(2\Lambda_1 + \Delta^2\Lambda_2\right) w_{A,x} & 0 \\
0 & \begin{array}{l} -2\Lambda_6 - \Delta^2\Lambda_7 \\ -\Delta\Lambda_8 \, \delta_{iM} \end{array} & \begin{array}{l} -\Delta^2\Lambda_9 - \Delta^2\Lambda_{10} w_{A,xx} \\ -\Delta\Lambda_{11} \, \delta_{iM} \end{array} & 0 \\
0 & \begin{array}{l} \Delta^2\Lambda_9 - \Delta^2\Lambda_{14} w_{A,xx} \\ + \Delta\Lambda_{11} \, \delta_{iM} \end{array} & \begin{array}{l} + 2\Lambda_{15} + \Delta^2\Lambda_{18} - \left(2 + \Delta^2\Lambda_{19}\right)\hat{N}_x \\ + \left(\Delta^2\Lambda_{20} - 2\Lambda_{16}\right) w_{A,xx} + \Delta^2\Lambda_{21} w_A \\ + \left(\frac{2\Lambda_{17}}{\Delta} + \Delta\Lambda_{22} + \Delta\Lambda_{23} w_A\right) \delta_{iM} \end{array} & 2 \\
0 & 0 & -2\bar{D}_x - \Delta^2\Lambda_{24} & \Delta^2
\end{bmatrix}
$$

$$C_i = \begin{bmatrix} \Lambda_1 & \dfrac{\Delta\Lambda_3}{2} & \left(w_{A,x} + \dfrac{\Delta}{2} w_{A,xx}\right)\Lambda_1 + \dfrac{\Delta\Lambda_4}{2} & \dfrac{\Delta\Lambda_5}{2} \\ -\dfrac{\Delta\Lambda_3}{2} & \Lambda_6 & -\dfrac{\Delta\Lambda_3 w_{A,x}}{2} & 0 \\ \dfrac{\Delta}{2}\left(\Lambda_{12} - \Lambda_{13} w_{A,xx}\right) & 0 & \begin{array}{l} -\Lambda_{15} + \hat{N}_x + \Lambda_{16} w_{A,xx} \\ + \dfrac{\Delta}{2}\left(\Lambda_{12} - \Lambda_{13} w_{A,xx}\right) w_{A,x} \\ + \dfrac{\Lambda_{17}}{\Delta}\left(\dfrac{\delta_{(i-1)M}}{4} - \delta_{iM} - \dfrac{\delta_{(i+1)M}}{4}\right) \end{array} & -1 \\ -\dfrac{\Delta\Lambda_{16}}{2} & 0 & \bar{D}_x - \dfrac{\Delta\Lambda_{16} w_{A,x}}{2} & 0 \end{bmatrix} \tag{55}$$

where i is the finite difference station and the subscript M of the Kronecker delta is as defined by equation (33). In writing the matrix difference equations (54), the ring properties are again assumed to be averaged over one difference spacing Δ as in the prebuckling solution. Also, as in the prebuckling solution, the boundary conditions give the additional equations needed in order to have the same number of unknowns as there are equations.

From equations (27), the boundary conditions on the buckling displacements for classical simple support boundary conditions are

$$N_{x_B} = 0$$
$$v_B = 0$$
$$w_B = 0$$
$$M_{x_B} = 0 \tag{56}$$

Substituting equations (51) and writing in finite difference form, the boundary conditions can be written in matrix form as follows:

At station $i = 0$ $(x = 0)$

$$\bar{A}_o\, Z_{B_{-1}} + \bar{B}\, Z_{B_o} + \bar{C}_o\, Z_{B_1} = 0 \tag{57}$$

and at station $i = k$ $(x = a)$

$$\bar{A}_k\, Z_{B_{k-1}} + \bar{B}\, Z_k + \bar{C}_k\, Z_{B_{k+1}} = 0 \tag{58}$$

where

$$Z_{B_i} = \begin{bmatrix} U_i \\ V_i \\ W_i \\ M_i \end{bmatrix}$$

$$\bar{A}_{o(k)} = \begin{bmatrix} -\dfrac{\Delta\Lambda_{13}}{2} & 0 & -\dfrac{\Delta\Lambda_{13} w_{A,x}}{2} - \Lambda_{16} & 0 \\ 0 & 0 & 0 & 0 \\ 0 & 0 & 0 & 0 \\ 0 & 0 & 0 & 0 \end{bmatrix}$$

$$\bar{B} = \begin{bmatrix} 0 & \Delta^2\Lambda_{14} & \Delta^2\Lambda_{12} + 2\Lambda_{16} & 0 \\ 0 & 1 & 0 & 0 \\ 0 & 0 & 1 & 0 \\ 0 & 0 & 0 & 1 \end{bmatrix}$$

$$\bar{C}_{o(k)} = \begin{bmatrix} \frac{\Delta\Lambda_{13}}{2} & 0 & \frac{\Delta\Lambda_{13} w_{A,x}}{2} - \Lambda_{16} & 0 \\ 0 & 0 & 0 & 0 \\ 0 & 0 & 0 & 0 \\ 0 & 0 & 0 & 0 \end{bmatrix} \tag{59}$$

In the 4×4 matrix coefficient expressions (55) and (59), the prebuckling displacements and derivatives at each station are determined from the prebuckling solution (eqs. (43) through (47)). The matrix difference equations (54), (57), and (58) define a linear homogeneous system of equations which have a nontrival solution only if the determinant of the coefficient matrix equals zero. The lowest value of the $\hat{N}_x$ for which this determinant is zero represents the buckling load of the cylinder. This value is found by solving the matrix difference equations by the modified Gaussian elimination method of reference 11 which was described in the prebuckling solution.

That is, the first of equations (54) and equation (57) are solved for Z_{B_o} in terms of Z_{B_1} to give

$$Z_{B_o} = \left[- \bar{A}_o A_o^{-1} B_o + \bar{B} \right]^{-1} \left[\bar{A}_o A_o^{-1} C_o - \bar{C}_o \right] Z_{B_1} \tag{60}$$

The recurrence equation is of the form

$$Z_{B_i} = P_i \, Z_{B_{i+1}} \tag{61}$$

$$i = 0,1,\ldots k$$

and therefore, P_o can be determined as

$$P_o = \left[- \bar{A}_o A_o^{-1} B_o + \bar{B} \right]^{-1} \left[\bar{A}_o A_o^{-1} C_o - \bar{C}_o \right] \tag{62}$$

Now substituting $Z_{B_{i-1}} = P_{i-1} \, Z_{B_i}$ into the general equation (54) provides the result

$$P_i = - \left[A_i P_{i-1} + B_i \right]^{-1} C_i \tag{63}$$

$$i = 1,2,\ldots,k$$

where the initial value of P is given by equation (62). The last of equations (54) and equation (58) provide the result

$$\left[\bar{A}_k P_{k-1} P_k + \bar{B} P_k + \bar{C}_k \right] Z_{B_{k+1}} = 0 \tag{64}$$

Now if for a value of $\hat{N}_x$ the determinant of the coefficient of $Z_{B_{k+1}}$ in equation (64) is zero, then this zero is a zero of the coefficient matrix and the $\hat{N}_x$ represents a critical load of the cylinder. The above solution requires only the inversion of 4×4 matrices for the determination of the buckling load and therefore is well suited for high speed computers.

The actual solution on the computer is done in the following manner: initially an n, the number of circumferential waves, and an $\hat{N}_x$ are judiciously selected; the prebuckling displacement and derivatives at each station are then calculated for the selected $\hat{N}_x$ and the value of the determinant of equation (64) is calculated; $\hat{N}_x$ is then iterated until a zero of the determinant is determined; then n is changed and the above procedure is repeated to determine a new $\hat{N}_x$; the lowest value of $\hat{N}_x$ which is determined is then taken to be the buckling load. The initial values for n and $\hat{N}_x$ mentioned above were taken in most cases to be the values obtained from a classical solution (w_A = constant).

Solution of Buckling Equations for Smeared Rings

When the rings are assumed to be smeared out over the ring spacing, the buckling equations (26) and boundary conditions (27) are still applicable except that the stress and moment resultants defined by equations (27) are defined as follows:

$$N_{y_B} = \frac{E_y}{1 - \mu_x'\mu_y'} \left[v_{B,y} + \frac{w_B}{R} + \mu_x' \left(u_{B,x} + w_{A,x}\, w_{B,x} \right) \right]$$

$$+ \frac{E_r A_r}{l} \left(v_{B,y} + \frac{w_B}{R} - \bar{z}_r w_{B,yy} \right)$$

$$M_{y_B} = - \left[\frac{D_y}{1 - \mu_x \mu_y} \left(w_{B,yy} + \mu_x w_{B,xx} \right) + \frac{E_r I_r}{l} w_{B,yy} \right.$$

$$\left. - \frac{E_r A_r \bar{z}_r}{l} \left(v_{B,y} + \frac{w_B}{R} - \bar{z}_r\, w_{B,yy} \right) \right]$$

$$M_{xy_B} = \left(2D_{xy} + \frac{G_s J_s}{d} + \frac{G_r J_r}{l} \right) w_{B,xy} \tag{65}$$

and N_{x_B}, M_{x_B}, and N_{xy_B} are as previously defined by equations (27) and l is the ring spacing. Similar equations for stiffened cylinders are presented in reference 13 except that an isotropic shell is used in reference 13 where an orthotropic shell is considered herein. To solve the smeared ring buckling equations (26) for the simple support boundary conditions considered herein, the finite difference method is used as was described for discrete ring case. The procedure is exactly the same as previously described and equations (51) through (64) appear the same except for the following three changes: the prebuckling displacements and derivatives are given by the analytic solution of equation (49); the summation and the Dirac delta function $\left[\sum_{j=1}^{N} \delta(x - jl) \right]$ are replaced by $\frac{1}{l}$ in the buckling equations (52) (Λ_1 through Λ_{24} are defined the same); and the matrix coefficients (55) of equations (54) are defined as follows:

$$
A_i = \begin{bmatrix}
\Lambda_1 & -\dfrac{\Delta\Lambda_3}{2} & \left(w_{A,x} - \dfrac{\Delta}{2} w_{A,xx}\right)\Lambda_1 - \dfrac{\Delta}{2}\Lambda_4 & -\dfrac{\Delta\Lambda_5}{2} \\
\dfrac{\Delta\Lambda_3}{2} & \Lambda_6 & \dfrac{\Delta\Lambda_3}{2} w_{A,x} & 0 \\
\dfrac{\Delta}{2}\left(\Lambda_{13} w_{A,xx} - \Lambda_{12}\right) & 0 & \begin{array}{l} -\Lambda_{15} + \hat{N}_x + \Lambda_{16} w_{A,xx} \\ + \dfrac{\Delta}{2}\left(\Lambda_{13} w_{A,xx} - \Lambda_{12}\right) w_{A,x} \\ - \dfrac{\Lambda_{17}}{l} \end{array} & -1 \\
\dfrac{\Delta\Lambda_{16}}{2} & 0 & \bar{D}_x + \dfrac{\Delta\Lambda_{16} w_{A,x}}{2} & 0
\end{bmatrix}
$$

$$
B_i = \begin{bmatrix}
-2\Lambda_1 - \Delta^2\Lambda_2 & 0 & -\left(2\Lambda_1 + \Delta^2\Lambda_2\right) w_{A,x} & 0 \\
0 & \begin{array}{l} -2\Lambda_6 - \Delta^2\Lambda_7 \\ - \dfrac{\Delta^2\Lambda_8}{l} \end{array} & \begin{array}{l} -\Delta^2\Lambda_9 - \Delta^2\Lambda_{10} w_{A,xx} \\ - \dfrac{\Delta^2\Lambda_{11}}{l} \end{array} & 0 \\
0 & \begin{array}{l} \Delta^2\Lambda_9 \\ - \Delta^2\Lambda_{14} w_{A,xx} \\ + \dfrac{\Delta^2\Lambda_{11}}{l} \end{array} & \begin{array}{l} 2\Lambda_{15} + \Delta^2\Lambda_{18} - \left(2+\Delta^2\Lambda_{19}\right)\hat{N}_x \\ + \left(\Delta^2\Lambda_{20} - 2\Lambda_{16}\right) w_{A,xx} \\ + \Delta^2\Lambda_{21} w_A + 2\dfrac{\Lambda_{17}}{l} + \Delta^2\dfrac{\Lambda_{22}}{l} \\ + \dfrac{\Delta^2\Lambda_{23}}{l} w_A \end{array} & 2 \\
0 & 0 & -2\bar{D}_x - \Delta^2\Lambda_{24} & \Delta^2
\end{bmatrix} \qquad (66)
$$

$$
C_i = \begin{bmatrix}
\Lambda_1 & \dfrac{\Delta\Lambda_3}{2} & \left(w_{A,x} + \dfrac{\Delta}{2} w_{A,xx}\right)\Lambda_1 + \dfrac{\Delta\Lambda_4}{2} & \dfrac{\Delta\Lambda_5}{2} \\[2ex]
-\dfrac{\Delta\Lambda_3}{2} & \Lambda_6 & -\dfrac{\Delta\Lambda_3 w_{A,x}}{2} & 0 \\[2ex]
\dfrac{\Delta}{2}\left(\Lambda_{12} - \Lambda_{13} w_{A,xx}\right) & 0 & \begin{array}{l} -\Lambda_{15} + \hat{N}_x + \Lambda_{16} w_{A,xx} \\[1ex] -\dfrac{\Delta}{2}\left(\Lambda_{13} w_{A,xx} - \Lambda_{12}\right) w_{A,x} \\[1ex] -\dfrac{\Lambda_{17}}{l} \end{array} & -1 \\[6ex]
-\dfrac{\Delta\Lambda_{16}}{2} & 0 & \bar{D}_x - \dfrac{\Delta\Lambda_{16} w_{A,x}}{2} & 0
\end{bmatrix}
\tag{66}
$$

For the numerical computations the computer program for discrete rings is used with equations (66) now used for the matrix coefficients in place of equations (55) and with the prebuckling displacements given by equation (49). The same procedure of calculating the buckling load $\hat{N}_x$ is used.

The solution of the buckling equations for the case where the rings were assumed to be smeared out was obtained in order to evaluate and compare the effect of discrete rings. It was also of interest to compare the buckling loads obtained when exact prebuckling deformations are considered to buckling loads obtained when classical prebuckling deformations (w_A = constant) are assumed. For smeared rings, the buckling solutions assuming classical prebuckling deformations are presented in reference 3, and for discrete rings a Galerkin solution of the classical buckling equations is presented in appendix A.

Buckling Shapes

The shape of the buckling displacement along the axial direction was determined by employing the following procedure. The right hand side of equation (64) is set equal to an arbitrary constant vector $\bar{c}$ which is defined as follows:

$$\bar{c} = \begin{bmatrix} 0 \\ 0 \\ DET \\ 0 \end{bmatrix} \tag{67}$$

In equation (67), DET is the value of the determinant of the coefficient of $Z_{B_{k+1}}$ in equation (64). Equation (64) now becomes

$$\left[\bar{A}_k P_{k-1} P_k + \bar{B} P_k + \bar{C}_k \right] Z_{B_{k+1}} = \bar{c} \tag{68}$$

In equation (68) define the matrix of the coefficients of $Z_{B_{k+1}}$ in the following notation

$$\left[\bar{A}_k P_{k-1} P_k + \bar{B} P_k + \bar{C}_k \right] = \begin{bmatrix} a_{11} & a_{12} & a_{13} & a_{14} \\ a_{21} & a_{22} & a_{23} & a_{24} \\ a_{31} & a_{32} & a_{33} & a_{34} \\ a_{41} & a_{42} & a_{43} & a_{44} \end{bmatrix} \tag{69}$$

Now from equation (68) using notation of equation (69), the solution for each of the four elements of the column vector $Z_{B_{k+1}}$ can be obtained by applying Cramer's rule as

$$U_{k+1} = \begin{vmatrix} a_{12} & a_{13} & a_{14} \\ a_{22} & a_{23} & a_{24} \\ a_{42} & a_{43} & a_{44} \end{vmatrix}$$

$$V_{k+1} = -\begin{vmatrix} a_{11} & a_{13} & a_{14} \\ a_{21} & a_{23} & a_{24} \\ a_{41} & a_{43} & a_{44} \end{vmatrix}$$

$$W_{k+1} = \begin{vmatrix} a_{11} & a_{12} & a_{14} \\ a_{21} & a_{22} & a_{24} \\ a_{41} & a_{42} & a_{44} \end{vmatrix}$$

$$M_{k+1} = -\begin{vmatrix} a_{11} & a_{12} & a_{13} \\ a_{21} & a_{22} & a_{23} \\ a_{41} & a_{42} & a_{43} \end{vmatrix} \tag{70}$$

Equation (70) determines $Z_{B_{k+1}}$ and then the remaining Z_B's are calculated in reverse order using equation (61). Once the Z_B's have been calculated, the buckling displacements w_B at any station along the cylinder are known in terms of an arbitrary constant. The buckling displacements are then normalized by dividing each displacement by the absolute value of the maximum displacement thus giving the normalized buckling displacements $\frac{w_B}{|w_{B_{max}}|}$.

For all the computations a high speed digital computer was used. Furthermore, the computer program reduced the order of the matrix to a maximum of a 4×4, therefore, the available storage space of the computer did not affect the limit on the number of stations along the length that could be used. For the calculations, the number of stations was increased until an increase in the number of stations did not affect the accuracy of the buckling load to within the accuracy for which the buckling load was obtained. Generally it was found that approximately 200 to 300 stations along the length of the shell were required for proper convergence.

In appendix B, the Fortran IV source program for the determination of the prebuckling displacements and buckling loads of a cylinder with discrete rings is listed.

The results of all the calculations are presented in the next section.

VIII. RESULTS AND DISCUSSION

General

Because of the large number of geometric and physical parameters involved in this investigation, it is impractical to present results of a general nature. However, it is of value to present some computed results for cylinders of contemporary proportions in order to study the influence of discrete ring stiffeners, prebuckling deformations and eccentrically applied compressive load resultants (applied edge moments). Therefore, computations of compressive buckling loads were made for two types of stiffened cylinders appropriate for large-diameter booster interstage structures: ring- and stringer-stiffened isotropic cylinders and ring-stiffened corrugated cylinders. For the computations, the material in the cylindrical shell and the material in the stiffeners were taken to be identical, a value of 0.32 was assigned to Poisson's ratio for the stiffened isotropic cylinders, and the elastic shell constants given by table I were assigned to the orthotropic shell constants for the corrugated cylinder. The dimensions of the cylinders are given in figure 2. Eccentricity effects of the stiffeners were studied by moving the stiffeners from the internal to the external surface of the shell.

The ring- and stringer-stiffened cylinders and the corrugated cylinders are susceptible to buckling modes of panel instability or general instability depending upon the number of rings on the cylinder and eccentricity of the stiffeners. General instability is defined as the buckling mode in which the rings deform radially and the cylinder wall and rings buckle as a composite wall. Panel instability is defined as the buckling mode in which the rings have little or no radial deformation and the cylinder buckles between rings. For the calculations the number of rings on these cylinders was varied and nondimensional buckling loads $\frac{\hat{N}_x}{E_x}$ or $\frac{\hat{N}_x}{E\bar{t}}$ $\left(\text{where } \bar{t} \text{ is the effective thickness of the isotropic cylinder wall, } \frac{A_s}{d} + t\right)$ were calculated for three cases: discrete rings taking into account prebuckling deformations (eqs. (43) through (47) and eqs. (62) through (64)); smeared rings taking into account prebuckling deformations (eq. (49) and eqs. (62) through (64) using matrix coefficients of eqs. (66)); and discrete rings assuming classical prebuckling deformations (eq. (A-8)). Calculations were also made by employing the theory of reference 3 (eq. (15)) which is a classical buckling theory, that is, assumes classical prebuckling deformations. For these calculations, general instability represents the case where the rings are smeared out and panel instability is taken to be the buckling load which is obtained by assuming the length of the cylinder is equal to the ring spacing.

The results of the computations are presented in tables II through V and in figures 3 through 11. Details and discussion of the computed results follow.

Buckling Predictions

The nondimensional buckling loads for ring- and stringer-stiffened isotropic cylinders and for ring-stiffened corrugated cylinders are presented in tables II and III and are shown in figures 3, 4, and 5. The calculated values in the tables are given for the governing mode of buckling, panel or general instability (panel instability values are denoted by an asterisk). In the figures, the nondimensional buckling load $\frac{\hat{N}_x}{Et}$ for ring- and stringer-stiffened cylinders and $\frac{\hat{N}_x}{E_x}$ for corrugated cylinders, is plotted against the number of rings N on the cylinder. The buckling loads for $N = 0$ correspond to buckling of a cylinder with no rings on it. For the calculations presented in tables II and III and figures 3, 4, and 5, the stiffened cylinders are assumed to have the compressive load applied at the middle surface of the cylindrical shell ($\bar{e} = 0$), therefore, the prebuckling state has the equivalent moment boundary condition as the buckling state $\left(M_{x_A} = M_{x_B} = 0\right)$. Calculations for eccentrically applied compressive loads (various $\bar{e}$'s) are presented in tables IV and V and are shown in figures 6 and 7.

For the external ring- and external stringer-stiffened isotropic cylinders, the computed results presented in table II and shown in figure 3 indicate that taking into account prebuckling deformations can cause the buckling load to be increased by as much as 77 percent for panel instability modes and to be decreased by as much as 21 percent for general instability modes of that predicted by classical theory. The increase in the panel instability buckling load results from assuming that the load is applied at the middle surface of the cylinder while classical theory implies that the load on the cylinder is applied at a distance which will insure constant prebuckling deformations. For a more complete discussion on the implications of classical theory, see the appendix of reference 13. The sensitivity of the buckling load upon the distance from the middle surface to the line where the applied load acts is shown in figures 6 and 7. The externally stiffened cylinder results also show that when prebuckling deformations are taken into account in the analysis, the buckling loads obtained by considering the rings discretely are as much as 9 percent less than the loads obtained by considering the rings smeared out (compare the general instability predictions in table II). Additional general instability calculations, not presented because general instability was not the governing mode of buckling, showed that a maximum difference in buckling loads of 10 percent between discrete and smeared out rings occurred for a cylinder with 1 ring. Using classical buckling theory, the difference in buckling loads between discrete and smeared out rings was negligible (see table II). Note also that when prebuckling deformations are taken into account the transition between panel and general instability occurs between a cylinder stiffened with 2 rings and one with 3 rings and that when classical prebuckling deformations are assumed this transition occurs between a cylinder stiffened with 3 rings and one with 4 rings.

For the internal ring- and internal stringer-stiffened isotropic cylinders, the computed results presented in table II and shown in figure 4 indicate that by taking into account prebuckling deformations and considering the rings discretely, the cylinders buckle in panel instability buckling modes and, therefore, significantly change the buckling modes of the cylinder from those predicted by classical theory. Also, the predicted buckling load is reduced from 61 to 20 percent of that predicted by classical theory. For general instability buckling modes, the computed results for smeared rings indicate that by taking into account prebuckling deformations the buckling load is reduced from 8 to 6 percent of that predicted by classical theory. Additional general instability calculations made for cylinders with one discrete ring but were not presented because general instability was not the governing mode of buckling. These calculations showed a maximum difference in buckling loads of 10 percent between the discrete and the smeared out ring.

For the ring-stiffened corrugated cylinders studied, the computed results presented in table III are shown in figure 5 indicate that the effect of prebuckling deformations on the buckling load is negligible. This result is as expected since for an axial compressed cylinder prebuckling deformations are proportional to Poisson's ratio and for a corrugated cylinder the value of the extensional circumferential Poisson's ratio ($\mu_y{}'$) is very small (see table I). The results for corrugated cylinders also show negligible effects due to discrete rings.

The influence of the eccentric distance of the applied compressive load on the buckling load is presented in tables IV and V and is shown in figures 6 and 7 for stiffened isotropic cylinders. In the figures the nondimensional buckling load $\frac{\hat{N}_x}{E\bar{t}}$ is plotted against the nondimensional distance $\frac{\bar{e}}{h}$, where $\bar{e}$ is the distance from cylinder's middle surface to the line on which the applied load $\hat{N}_x$ acts and h is one-half the height of the stringer (see figure 2). An eccentric applied compressive load is equivalent to a loading combination of an axial compressive load applied at the middle surface of the cylinder plus an axisymmetric end moment.

For an internal ring- and internal stringer-stiffened isotropic cylinder, the results presented in table IV and shown in figure 6 show that when the cylinder is loaded at an $\frac{\bar{e}}{h}$ of -1.1, the general instability buckling load is increased 21 percent over the buckling load obtained when the cylinder is loaded at its middle surface $\left(\frac{\bar{e}}{h} = 0\right)$. This increase or decrease in load is an interesting phenomenon for it shows that a stiffened cylinder has a maximum buckling load which depends upon the position where the load is introduced into the cylinder. The prebuckling and buckling shapes corresponding to this cylinder and loadings are presented in figure 9.

In table V and figure 7, computed results for eccentrically applied compressive loads are presented for internal and external stringer-stiffened isotropic cylinders. The same phenomenon observed in figure 6 is also observed in figure 7 for these cylinders. However, the buckling loads for these cylinders are increased as much as 6 times depending upon the position where the load is applied at the ends of the cylinder, thus showing the sensitivity at these cylinders to where the load is applied. The prebuckling and buckling shapes for these cylinders are presented in figures 10 and 11.

Prebuckling and Buckling Shapes

In figures 8 through 11, representative axial prebuckling and buckling shapes are shown for the stiffened isotropic cylinders previously presented. In the figures, the prebuckling deformation w_A or the normalized buckling deformation $\frac{w_B}{|w_{B_{max}}|}$ is plotted against the cylinder length $\frac{x}{a}$.

In figure 8, prebuckling and buckling shapes illustrating panel instability and general instability modes of buckling are shown for an internally stiffened cylinder with 4 rings presented in figure 4. For this cylinder panel instability is the governing mode of buckling. The prebuckling shapes (figure 8(a)) show that internal stiffening causes the prebuckling deformations to be negative near the ends of the cylinder. This prebuckling shape is quite different from the usual prebuckling shape of Föppl shape experienced in unstiffened cylinders (ref. 14). The buckling shapes shown in figure 8(b) illustrate the panel instability and the general instability modes of buckling.

Prebuckling shapes and buckling shapes are shown in figures 9, 10, and 11 for the cylinders presented in figures 6 and 7. These figures illustrate how the prebuckling and buckling shapes are influenced due to eccentrically applied loads.

IX. CONCLUDING REMARKS

An analytical investigation has been presented on the buckling of eccentrically stiffened orthotropic cylinders in which discretely located ring stiffeners and prebuckling deformations are included in the analysis. Nonlinear prebuckling equations and boundary conditions and linear buckling equations and boundary conditions have been derived by using energy principles.

Solutions of the prebuckling and buckling equations which satisfy classical simple support boundary conditions have been obtained by the method of finite differences for cylinders loaded with any combination of axial compression and lateral pressure. The finite difference method of solution which was used employed a reduction of the governing equations to a second order system of equations, a matrix formulation of the finite difference equations, and a modified Gaussian elimination procedure of solution. For comparison similar type solutions were presented for the case where the rings were assumed to be smeared out. Also in appendix A, a Galerkin solution was presented for the classical buckling problem of a cylinder with discrete rings.

Sample calculations have been shown for two types of contemporary stiffened cylinders in order to illustrate the importance of prebuckling deformations, discrete rings and eccentrically applied compressive loads.

The calculations presented show that by taking into account prebuckling deformations the following changes in the predicted buckling load may result.

1. The buckling load may be substantially increased or decreased of that predicted by classical theory.

2. The buckling load may be decreased for cylinders with few rings by considering the rings discretely located.

3. The transition between panel and general instability modes of buckling is changed from that predicted by classical theory.

4. The buckling load may be substantially increased or decreased (as much as 6 times for the cylinders studied) depending upon the position of the compressive load applied at the ends of the cylinder.

In conclusion, this research has improved the theoretical understanding of the buckling of stiffened cylinders; thus, it has supplied a means for achieving better agreement between theory and experiment.

X. ACKNOWLEDGMENTS

The author wishes to express his thanks to the National Aeronautics and Space Administration and to Mr. James P. Peterson for permitting him to perform this research as part of his work assignment at Langley Research Center; and to Dr. Daniel Frederick, Professor of Engineering Mechanics, Virginia Polytechnic Institute, for his direction and guidance.

XI. REFERENCES

1. Van der Neut, A.: The General Instability of Stiffened Cylindrical Shells Under Axial Compression. Rept. S. 314, National Aeronautics Research Institute (Amsterdam), 1947.

2. Baruch, M.; and Singer, J.: Effect of Eccentricity of Stiffeners on the General Instability of Stiffened Cylindrical Shells Under Hydrostatic Pressure. J. Mech. Eng. Sci., Vol. 5, No. 1, 1963, pp. 23 - 27.

3. Block, David L.; Card, Michael F.; and Mikulas, Martin M., Jr.: Buckling of Eccentrically Stiffened Orthotropic Cylinders. NASA TN D-2960, 1965.

4. Hedgepeth, John M.; and Hall, David B.: Stability of Stiffened Cylinders. AIAA Paper No. 65-79 presented at Second Aerospace Sciences meeting, New York, N. Y., Jan. 25 - 27, 1965.

5. DeLuzio, A. J.; Stuhlman, C. E.; and Almroth, B. O.: Influence of Stiffener Eccentricity and End Moment on the Stability of Cylinders in Compression. Proceedings of the AIAA 6th Structures and Materials Conference, Palm Springs, 5-7 April 1965, pp. 117 - 123.

6. Card, Michael F.: Preliminary Results of Compression Tests on Cylinders with Eccentric Longitudinal Stiffeners. NASA TM X-1004, 1964.

7. Peterson, James P.; and Anderson, James Kent: Bending Tests of Large-Diameter Ring-Stiffened Corrugated Cylinders. NASA TN D-3336, 1966.

8. Stein, Manuel: The Influence of Prebuckling Deformations and Stresses on the Buckling of Perfect Cylinders. NASA TR T-190, 1964.

9. Almroth, B. O.: Influence of Edge Conditions on the Stability of Axially Compressed Cylindrical Shells. NASA CR-161, 1965.

10. Block, David L.: Influence of Ring Stiffeners on Instability of Orthotropic Cylinders in Axial Compression. NASA TN D-2482, 1964.

11. Budiansky, B.; and Radkowski, P. P.: Numerical Analysis of Unsymmetrical Bending of Shells of Revolution. AIAA Jour., Vol. 1, No. 8, August 1963, pp. 1833 - 1842.

12. Stein, Manuel; and Mayers, J.: A Small-Deflection Theory for Curved Sandwich Plates. NACA Rept. 1008, 1951. (supersedes NACA TN 2017.)

13. McElman, John A.; Mikulas, Martin M., Jr.; and Stein, Manuel: Static and Dynamic Effects of Eccentric Stiffening of Plates and Cylindrical Shells. AIAA Paper No. 65-370 presented at AIAA Second Annual Meeting, San Francisco, California, July 26-29, 1965.

14. Föppl, L.: Achsensymmetrisches Ausknicken Zylindrischer Schalen. S. - B. Bayr. Akad. Wiss. 1926, pp. 27-40.

The vita has been removed from the scanned document

XIII. APPENDIX A

When the classical prebuckling displacement state is assumed, that is, w_A = constant, the classical theory buckling equations for a stiffened orthotropic cylinder with discrete rings can be determined from equations (26) as

$$N_{x_{B,x}} + N_{xy_{B,y}} = 0$$

$$N_{y_{B,y}} + N_{xy_{B,x}} = 0$$

$$-M_{x_{B,xx}} + M_{xy_{B,xy}} - M_{y_{B,yy}} + \frac{N_{y_B}}{R} + \hat{N}_x \, w_{B,xx} + pR \, w_{B,yy} = 0 \tag{A-1}$$

with boundary conditions of

$$N_{x_B} = 0 \quad \text{or} \quad u_B = 0$$

$$N_{xy_B} = 0 \quad \text{or} \quad v_B = 0$$

$$M_{x_B} = 0 \quad \text{or} \quad w_{B,x} = 0$$

$$M_{x_{B,x}} - M_{xy_{B,y}} - \hat{N}_x \, w_{B,x} = 0 \quad \text{or} \quad w_B = 0 \tag{A-2}$$

where

$$N_{x_B} = \frac{E_x}{1 - \mu_x'\mu_y'}\left[u_{B,x} + \mu_y'\left(v_{B,y} + \frac{w_B}{R}\right)\right] + \frac{E_sA_s}{d}\left(u_{B,x} - \bar{z}_s\, w_{B,xx}\right)$$

$$N_{y_B} = \frac{E_y}{1 - \mu_x'\mu_y'}\left(v_{B,y} + \frac{w_B}{R} + \mu_x'\, u_{B,x}\right) + \sum_{j=1}^{N} \delta(x - jl)\, E_rA_r\Big(v_{B,y}$$

$$+ \frac{w_B}{R} - \bar{z}_r\, w_{B,yy}\Big)$$

$$N_{xy_B} = G_{xy}\left(u_{B,y} + v_{B,x}\right)$$

$$M_{x_B} = -\Bigg[\frac{D_x}{1 - \mu_x\mu_y}\left(w_{B,xx} + \mu_y\, w_{B,yy}\right) + \frac{E_sI_s}{d}\, w_{B,xx} - \frac{E_sA_s\bar{z}_s}{d}\Big(u_{B,x}$$

$$- \bar{z}_s\, w_{B,xx}\Big)\Bigg]$$

$$M_{y_B} = -\Bigg\{\frac{D_y}{1 - \mu_x\mu_y}\left(w_{B,yy} + \mu_x\, w_{B,xx}\right) + \sum_{j=1}^{N} \delta(x - jl)\Big[E_rI_r\, w_{B,yy}$$

$$- E_rA_r\bar{z}_r\left(v_{B,y} + \frac{w_B}{R} - \bar{z}_r\, w_{B,yy}\right)\Big]\Bigg\}$$

$$M_{xy_B} = \left[2D_{xy} + \frac{G_sI_s}{d} + \sum_{j=1}^{N} \delta(x - jl)\, G_rJ_r\right] w_{B,xy} \qquad \text{(A-3)}$$

and $\hat{N}_x$ is the compressive load, $N_{y_A} = -pR$ and $N_{xy_A} = 0$.

To obtain a solution for the buckling load and to satisfy the boundary conditions (A-2) of classical simple support $\left(v_B = N_{xB} = M_{xB} = w_B = 0\right)$ considered herein, the buckling displacements are taken as

$$u_B = \cos\frac{ny}{R}\sum_{q=1}^{\infty} c_q \cos\frac{q\pi x}{a}$$

$$v_B = \sin\frac{ny}{R}\sum_{q=1}^{\infty} b_q \sin\frac{q\pi x}{a}$$

$$w_B = \cos\frac{ny}{R}\sum_{q=1}^{\infty} a_q \sin\frac{q\pi x}{a} \tag{A-4}$$

where n is the number of circumferential waves and the coefficients a_q, b_q, and c_q are to be determined.

By use of the Galerkin method, the following set of equations for the unknown coefficients a_q, b_q, and c_q must be satisfied.

$$\int_0^{2\pi R}\int_0^{a} Q_x\,(u,v,w)\,\cos\frac{sy}{R}\,\cos\frac{r\pi x}{a}\,dxdy = 0$$

$$\int_0^{2\pi R}\int_0^{a} Q_y\,(u,v,w)\,\sin\frac{sy}{R}\,\sin\frac{r\pi x}{a}\,dxdy = 0$$

$$\int_0^{2\pi R}\int_0^{a} Q_z\,(u,v,w)\,\cos\frac{sy}{R}\,\sin\frac{r\pi x}{a}\,dxdy = 0 \tag{A-5}$$

$$s = 0,\ 1,\ 2\ \cdots$$

$$r = 1,\ 2,\ 3\ \cdots.$$

where Q_x, Q_y, and Q_z are the result of substituting the series for the buckling displacements u, v, and w, equations (A-4), into the governing equations (A-1).

From equations (A-5) the resulting system of equations is determined as

$$-F_1\, c_r + F_2\, b_r + F_3\, a_r = 0$$

$$F_2\, c_r - F_4\, b_r - \frac{2F_5}{a} \sum_{j=1}^{N} \sin \frac{r\pi j}{N+1} \sum_{q=1}^{\infty} b_q \sin \frac{q\pi j}{N+1}$$
$$- F_6\, a_r - \frac{2F_7}{a} \sum_{j=1}^{N} \sin \frac{r\pi j}{N+1} \sum_{q=1}^{\infty} a_q \sin \frac{q\pi j}{N+1} = 0$$

$$F_3\, c_r - F_6\, b_r - \frac{2F_7}{a} \sum_{j=1}^{N} \sin \frac{r\pi j}{N+1} \sum_{q=1}^{\infty} b_q \sin \frac{q\pi j}{N+1}$$
$$- \left[F_8 - N_x \left(\frac{r\pi}{a}\right)^2 - pR \left(\frac{n}{R}\right)^2\right] a_r$$
$$- \frac{2\left(F_9 + F_{10}\right)}{a} \sum_{j=1}^{N} \sin \frac{r\pi j}{N+1} \sum_{q=1}^{\infty} a_q \sin \frac{q\pi j}{N+1}$$
$$- \frac{2F_{11}}{a} \sum_{j=1}^{N} \left(\frac{r\pi}{a}\right) \cos \frac{r\pi j}{N+1} \sum_{q=1}^{\infty} a_q \left(\frac{q\pi}{a}\right) \cos \frac{q\pi j}{N+1} = 0 \qquad \text{(A-6)}$$

$$r = 1, 2, \cdots\cdots$$

where

$$F_1 = \left(\frac{E_x}{1 - \mu_x'\mu_y'} + \frac{E_sA_s}{d}\right)\left(\frac{r\pi}{a}\right)^2 + G_{xy}\left(\frac{n}{R}\right)^2$$

$$F_2 = \left(\frac{E_x\ \mu_y'}{1 - \mu_x'\mu_y'} + G_{xy}\right)\left(\frac{r\pi}{a}\right)\left(\frac{n}{R}\right)$$

$$F_3 = \frac{E_x\ \mu_y'}{R\left(1 - \mu_x'\mu_y'\right)}\left(\frac{r\pi}{a}\right) + \frac{E_sA_s\bar{z}_s}{d}\left(\frac{r\pi}{a}\right)^3$$

$$F_4 = \frac{E_y}{1 - \mu_x'\mu_y'}\left(\frac{n}{R}\right)^2 + G_{xy}\left(\frac{r\pi}{a}\right)^2$$

$$F_5 = E_rA_r\left(\frac{n}{R}\right)^2$$

$$F_6 = \frac{E_y\ n}{R^2\left(1 - \mu_x'\mu_y'\right)}$$

$$F_7 = E_rA_r\ \frac{n}{R}\left[\frac{1}{R} + \bar{z}_r\left(\frac{n}{R}\right)^2\right]$$

$$F_8 = \left(\frac{D_x}{1 - \mu_x \mu_y} + \frac{E_s I_s}{d} + \frac{E_s A_s \bar{z}_s^{\,2}}{d} \right) \left(\frac{r\pi}{a}\right)^4 + \left(\frac{2D_x \mu_y}{1 - \mu_x \mu_y} + 2D_{xy} + \frac{G_s I_s}{d} \right) \left(\frac{n}{R}\right)^2 \left(\frac{r\pi}{a}\right)^2 + \frac{D_y}{1 - \mu_x \mu_y} \left(\frac{n}{R}\right)^4 + \frac{E_y}{R^2 \left(1 - \mu_x' \mu_y'\right)}$$

$$F_9 = E_r I_r \left(\frac{n}{R}\right)^4$$

$$F_{10} = E_r A_r \left[\left(\frac{1}{R}\right)^2 + \frac{2\bar{z}_r n^2}{R^3} + \bar{z}_r^{\,2} \left(\frac{n}{R}\right)^4 \right]$$

$$F_{11} = G_r J_r \left(\frac{n}{R}\right)^2 \qquad \text{(A-7)}$$

and where the reciprocal relations $\mu_x' E_y = \mu_y' E_x$ and $\mu_x D_y = \mu_y D_x$ have been employed to simplify the equations. Equations (A-6) give the criteria for buckling if the determinant of the coefficients vanish, that is

$$\left| A_{rq} \right| = 0$$

By combining equations (A-6), the following determinant of the coefficients a_r can be obtained

$$\left| A_{rq} \right| = \left| \left\{ F_8 + \left(F_9 + F_{10}\right) \Phi_r + F_{11} \Psi_r \right. \right.$$

$$+ F_3 \left[\frac{F_2 \left(F_6 + F_7 \Phi_r\right) - F_3 \left(F_4 + F_5 \Phi_r\right)}{F_1 \left(F_4 + F_5 \Phi_r\right) - F_2^2} \right]$$

$$+ \left(F_6 + F_7 \Phi_r\right) \left[\frac{F_3 F_2 - F_1 \left(F_6 + F_7 \Phi_r\right)}{F_1 \left(F_4 + F_5 \Phi_r\right) - F_2^2} \right] - \hat{N}_x \left(\frac{r\pi}{a}\right)^2$$

$$\left. - pR \left(\frac{n}{R}\right)^2 \right\} \delta_{rq} + F_9 \Phi_{rq} + F_{11} \Psi_{rq} \Bigg| = 0 \qquad (A\text{-}8)$$

$$r = 1, 2, \cdots$$

$$q = 1, 2, \cdots$$

where

$$\Phi_r = \frac{2}{a} \sum_{j=1}^{N} \sin^2 \frac{r\pi j}{N+1}$$

$$\Phi_{rq} = \frac{2}{a} \sum_{j=1}^{N} \sin \frac{r\pi j}{N+1} \sin \frac{q\pi j}{N+1}$$

$$\Psi_r = \frac{2}{a} \sum_{j=1}^{N} \left(\frac{r\pi}{a}\right)^2 \cos^2 \frac{r\pi j}{N+1}$$

$$\Psi_{rq} = \frac{2}{a} \sum_{j=1}^{N} \left(\frac{r\pi}{a}\right) \left(\frac{q\pi}{a}\right) \cos \frac{r\pi j}{N+1} \cos \frac{q\pi j}{N+1} \qquad (A\text{-}9)$$

and F's are as defined by equation (A-7).

Examination of the determinant given by equation (A-8) reveals that the terms with r and q odd are not coupled with the terms r and q even. Thus, the determinant of equation (A-8) may be separated into two determinants, one for r and q odd, and one for r and q even. The determinant for r and q odd represents a symmetrical w-deformation and the determinant for r and q even represents an antisymmetrical w-deformation. The form of these two determinants is identical to the determinant of equation (A-8) except for the mentioned restrictions on r and q. Each determinant given by equation (A-8) (r and q odd, or r and q even) is in the form of a standard eigenvalue problem and is solved on a high speed computer. When computing the buckling load, each determinant is minimized numerically for integral values of n, the number of circumferential waves in the buckle pattern and the buckling load is taken to be the absolute minima obtained from the r and q odd determinant and the r and q even determinant. The size of the determinants (r) is determined by requiring that the buckling load converges to a desired accuracy. For the calculations presented herein, the size of the determinants was increased until the buckling load between a specified order determinant and a determinant of one less order did not vary to within the accuracy of the calculations.

All numerical calculations presented were performed on an electronic computer.

XIV. APPENDIX B

In this section, the Fortran IV source program is listed for the determination of the prebuckling displacements and buckling loads of an eccentrically stiffened orthotropic cylinder with discretely located rings.

```
  1 FORMAT(94H BUCKLING OF SIMPLY-SUPPORTED CYLINDER WITH DISCRETE RIN
   1GS, INCLUDING PREBUCKLING DEFORMATIONS/20H BLOCK RDF 313 PN A880)
  2 FORMAT(////)
  3 FORMAT(7(2XE16.8))
  4 FORMAT(6E12.5)
  5 FORMAT(F5.0,5E12.5)
  6 FORMAT(//15H DISCRETE RINGS)
102 FORMAT(//2X19HCYLINDER PROPERTIES//3X4HMUX=E11.4,5X3HDX=E11.4/3X4H
   1MUY=E11.4,5X3HDY=E11.4/2X5HMUXP=E11.4,4X4HDXY=E11.4/2X5HMUYP=E11.4
   2,5X3HEX=E11.4/5X2HR=E11.4,5X3HEY=E11.4/5X2HA=E11.4,4X4HGXY=E11.4/2
   3X5HPRES=E11.4,6X2HE=E11.4)
103 FORMAT(//2X15HRING PROPERTIES//4X3HER=E11.4,3X5HGRJR=E11.4/4X3HAR=
   1E11.4,5X3HZR=E11.4/4X3HIR=E11.4,6X2HN=E11.4)
104 FORMAT(//2X19HSTRINGER PROPERTIES//4X3HES=E11.4,3X5HGSJS=E11.4/4X3
   1HAS=E11.4,5X3HZS=E11.4/4X3HIS=E11.4,6X2HD=E11.4)
105 FORMAT(//2X24HSTATIONS BETWEEN RINGS =,F5.0)
    REAL IS,IR,NX,NXO,NI
    DIMENSION H(2),L(99),F(2,2),FCOF(2,2),P(500,4,4),Q(500,4),X(2,2),
   1Y(2),ZBAR(500,2),DWA(500),DDWA(500),WA(500),ABARO(4,4),ABARF(4,4)
   2,BBAR(4,4),CBARO(4,4),CBARF(4,4),A1(4,4),B1(4,4),CZ(4,4),IPIVOT(4)
   3,INDEX(4,2),A11(4,4),B11(4,4),A12(4,4),B12(4,4),BZZ(4,1),L1(99),L2
   4(99),A3(4,4)
    WRITE(6,1)
    WRITE(6,6)
100 READ(5,5)NI,NXO,PRES,E,CIRNI
    READ(5,4)UX,UY,UXP,UYP,DX,DY,DXY,EY,EX,GXY,R,AA
    READ(5,4)ES,AS,IS,ZS,D,GSJS
    READ(5,4)ER,AR,IR,ZR,CAPN,GRJR
    WRITE(6,102)UX,DX,UY,DY,UXP,DXY,UYP,EX,R,EY,AA,GXY,PRES,E
    WRITE(6,103)ER,GRJR,AR,ZR,IR,CAPN
    WRITE(6,104)ES,GSJS,AS,ZS,IS,D
    WRITE(6,105)NI
    DELNX1=10.
    DELNX2=-1.
    PI=3.1415926
 CALCULATE NUMEROUS CONSTANTS
    ANXFIN=.999E38
    UXYP=1.-UXP*UYP
    EBX=EX/UXYP+ES*AS/D
    R5=DX/(1.-UX*UY)+ES*IS/D+ES*AS*ZS**2/D-(ES*AS*ZS/D)**2/EBX
    R2=(EY/(R*R*UXYP)-(EY*UXP)**2/(R*R*UXYP**2*EBX))/R5
```

```
      R3=ER*AR/(R**2*R5)
      DEL=AA/((CAPN+1.)*NI)
      CIRF=CIRNI+7.
      EAZ=ES*AS*ZS/D
      UXYQ=1.-UX*UY
      DBX=DX/UXYQ+ES*IS/D+EAZ*ZS
      R7=EY*UXP*EAZ/(EBX*UXYP)
      R8=EY/(R*UXYP)-(EY*UXP)**2/(R*EBX*UXYP**2)
      R9=EY*UXP/(EBX*UXYP)
      C1=EX/UXYP+ES*AS*(1.-EAZ*ZS/DBX)/D
      C5=EY*UXP/(R*UXYP)
      DO 213 I=1,4
      DO 213 J=1,4
      ABARO(I,J)=0.
      BBAR(I,J)=0.
      CBARO(I,J)=0.
      ABARF(I,J)=0.
  213 CBARF(I,J)=0.
      ABARO(1,1)=-DEL*EBX/2.
      ABARF(1,1)=ABARO(1,1)
      BBAR(1,3)=C5*DEL**2+2.*EAZ
      DO 214 I=2,4
  214 BBAR(I,I)=1.
      CBARO(1,1)=-ABARO(1,1)
      CBARF(1,1)=-ABARO(1,1)
      A1(1,1)=C1
      A1(1,4)=-DEL*EAZ/(2.*DBX)
      A1(2,2)=GXY
      A1(2,4)=0.
      A1(3,2)=0.
      A1(3,4)=-1.
      A1(4,1)=DEL*EAZ/2.
      A1(4,2)=0.
      A1(4,4)=0.
      B1(1,2)=0.
      B1(1,4)=0.
      DO 215 J=2,4
  215 B1(J,1)=0.
      B1(2,4)=0.
      B1(3,4)=2.
      B1(4,2)=0.
```

```
      B1(4,4)=DEL**2
      CZ(1,1)=C1
      CZ(2,2)=GXY
      CZ(2,4)=0.
      CZ(3,2)=0.
      CZ(3,4)=-1.
      CZ(1,4)=-A1(1,4)
      CZ(4,1)=-A1(4,1)
      CZ(4,2)=0.
      CZ(4,4)=0.
      DO 223 I=1,4
  223 BZZ(I,1)=1.
      CIRN=CIRNI
  252 ADA=CIRN/R
      MMM=1
      TESTNX=NX0*1.3
      NX=NX0
      C6=EY*ADA/(R*UXYP)
      C7=EX*UYP*ADA/UXYP
      C2=C5-EAZ*DX*UY*ADA**2/(UXYQ*DBX)
      C3=C7+GXY*ADA
      C4=ER*AR*ADA*(1./R+ZR*ADA**2)
      C9=(ER*IR+ER*AR*ZR**2)*ADA**4+2.*ER*AR*ZR*ADA**2/R+ER*AR/R**2
      GR=GRJR*ADA**2
      BBAR(1,2)=C7*DEL**2
      A1(2,1)=DEL*C3/2.
      A1(1,2)=-A1(2,1)
      B1(1,1)=-2.*C1-GXY*DEL**2*ADA**2
      B1(4,3)=-2.*DBX-DX*UY*ADA**2*DEL**2/UXYQ
      CZ(1,2)=A1(2,1)
      CZ(2,1)=A1(1,2)
  251 C8=DY*ADA**4/UXYQ+EY/(R**2*UXYP)-R9*ADA**2*NX
      IF(NX-TESTNX)255,244,244
  255 C10=ADA**2*(DY*UX/UXYQ+2.*DXY+GSJS/D)-NX
      IF(PRES)271,272,271
  271 PRES=2.*NX/R
      GO TO 272
  272 R6=NX*(E-ES*AS*ZS/(D*EBX))/R5
      R4=(-PRES+EY*UXP*NX/(R*UXYP*EBX))/R5
      R1=(2.*EY*UXP*ES*AS*ZS/(R*UXYP*EBX*D)+NX)/R5
      H(1)=R4*DEL**2
```

```
      H(2)=0.
      NCAP=CAPN
      K1=(NCAP+1)*IFIX(NI)
      ZBAR(K1,1)=R6
      ZBAR(K1,2)=0.
      K2=K1-1
      K3=K1+1
      DO 201 I1=1,NCAP
  201 L(I1)=I1*IFIX(NI)
      L(NCAP+1)=5000
      F(1,1)=-2.+R1*DEL**2
      F(2,2)=-2.
      F(2,1)=-DEL**2
      I1=1
      DO 200 I=1,K2
      IF(I-L(I1))203,204,203
  203 F(1,2)=DEL**2*R2
      GO TO 208
  204 F(1,2)=DEL**2*(R2+R3/DEL)
      I1=I1+1
  208 IF(I-1)300,301,300
  301 FCOF(1,1)=F(2,2)
      FCOF(1,2)=-F(1,2)
      FCOF(2,1)=-F(2,1)
      FCOF(2,2)=F(1,1)
      DET1=F(1,1)*F(2,2)-F(1,2)*F(2,1)
      DO 205 J=1,2
      DO 205 K=1,2
  205 P(I,J,K)=-FCOF(J,K)/DET1
      Q(1,1)=-P(1,1,1)*(R4*DEL**2-R6)
      Q(1,2)=-P(1,2,1)*(R4*DEL**2-R6)
      GO TO 200
  300 DO 206 J=1,2
      DO 206 K=1,2
  206 X(J,K)=P(I-1,J,K)+F(J,K)
      FCOF(1,1)=X(2,2)
      FCOF(1,2)=-X(1,2)
      FCOF(2,1)=-X(2,1)
      FCOF(2,2)=X(1,1)
      DET1=X(1,1)*X(2,2)-X(1,2)*X(2,1)
      DO 207 J=1,2
```

```
      DO 207 K=1,2
  207 P(I,J,K)=-FCOF(J,K)/DET1
      DO 209 J=1,2
  209 Y(J)=H(J)-Q(I-1,J)
      DO 210 K=1,2
  210 Q(I,K)=-P(I,K,1)*Y(1)-P(I,K,2)*Y(2)
  200 CONTINUE
      DO 211 K=1,K2
      K5=K1-K
      DO 211 J=1,2
  211 ZBAR(K5,J)=P(K5,J,1)*ZBAR(K5+1,1)+P(K5,J,2)*ZBAR(K5+1,2)+Q(K5,J)
      WA(1)=0.
      DO 233 I=1,K1
  233 WA(I+1)=ZBAR(I,2)
      DWA(1)=(2.*ZBAR(1,2)-R6*DEL**2)/(2.*DEL)
      DWA(2)=ZBAR(2,2)/(2.*DEL)
      DWA(K3)=(R6*DEL**2-2.*ZBAR(K2,2))/(2.*DEL)
      DDWA(1)=R6
      DDWA(2)=ZBAR(1,1)
      DDWA(K3)=R6
      DO 212 K=3,K1
      DWA(K)=(ZBAR(K,2)-ZBAR(K-2,2))/(2.*DEL)
  212 DDWA(K)=ZBAR(K-1,1)
      ABARO(1,3)=-DEL*EBX*DWA(1)/2.-EAZ
      ABARF(1,3)=-DEL*EBX*DWA(K3)/2.-EAZ
      CBARO(1,3)=DEL*EBX*DWA(1)/2.-EAZ
      CBARF(1,3)=DEL*EBX*DWA(K3)/2.-EAZ
      I1=1
      DO 250  I=1,K3
      A1(1,3)=C1*DWA(I)-DEL*(C1*DDWA(I)+C2)/2.
      A1(2,3)=A1(2,1)*DWA(I)
      A1(3,1)=-DEL*(C5-EBX*DDWA(I))/2.
      A1(4,3)=DBX+DEL*EAZ*DWA(I)/2.
      B1(1,3)=(-2.*C1-DEL**2*GXY*ADA**2)*DWA(I)
      CZ(1,3)=C1*DWA(I)+DEL*(C1*DDWA(I)+C2)/2.
      CZ(2,3)=-A1(2,3)
      CZ(3,1)=-A1(3,1)
      CZ(4,3)=DBX-DEL*EAZ*DWA(I)/2.
      CN1=-C10+EAZ*DDWA(I)
      CN2=DEL*(C5*DWA(I)-EBX*DWA(I)*DDWA(I))/2.
      CN3=2.*C10+DEL**2*C8+DDWA(I)*(-2.*EAZ+DEL**2*(R7*ADA**2-C5))+DEL**
```

```
   22*R8*ADA**2*WA(I)
      IF(I-L(I1))220,217,216
  217 A1(3,3)=CN1-CN2-GR/(4.*DEL)
      CZ(3,3)=CN1+CN2+GR/(4.*DEL)
      L1(I1)=L(I1)+1
      GO TO 222
  216 IF(I-L1(I1))218,219,218
  219 A1(3,3)=CN1-CN2-GR/DEL
      CZ(3,3)=CN1+CN2-GR/DEL
      B1(2,2)=-DEL**2*ADA**2*(EY/UXYP+ER*AR/DEL)-2.*GXY
      B1(2,3)=-DEL**2*(C6+GXY*ADA*DDWA(I)+C4/DEL)
      B1(3,2)=DEL**2*(C6-C7*DDWA(I)+C4/DEL)
      B1(3,3)=CN3+2.*GR/DEL+DEL*(C9+ER*AR*ADA**2*WA(I)/R)
      L2(I1)=L1(I1)+1
      GO TO 224
  218 IF(I-L2(I1))220,221,220
  221 A1(3,3)=CN1-CN2+GR/(4.*DEL)
      CZ(3,3)=CN1+CN2-GR/(4.*DEL)
      I1=I1+1
      GO TO 222
  220 A1(3,3)=CN1-CN2
      CZ(3,3)=CN1+CN2
      GO TO 222
  222 B1(2,2)=-DEL**2*EY*ADA**2/UXYP-2.*GXY
      B1(2,3)=-DEL**2*(C6+GXY*ADA*DDWA(I))
      B1(3,2)=DEL**2*(C6-C7*DDWA(I))
      B1(3,3)=CN3
      IF(I-1)224,225,224
  225 DO 260 M=1,4
      DO 260 K=1,4
  260 A3(M,K)=A1(M,K)
 (1)  CALL MATINV(A3,4,BZZ,0,DETERM,IPIVOT,INDEX,4,ISCALE)
      DO 226 M=1,4
      DO 226 J=1,4
      A11(M,J)=0.
      B11(M,J)=0.
      DO 226 K=1,4
      A11(M,J)=A11(M,J)+A3(M,K)*B1(K,J)
  226 B11(M,J)=B11(M,J)+A3(M,K)*CZ(K,J)
      DO 227 M=1,4
      DO 227 J=1,4
```

```
      A12(M,J)=0.
      B12(M,J)=0.
      DO 227 K=1,4
      A12(M,J)=A12(M,J)+ABARO(M,K)*A11(K,J)
  227 B12(M,J)=B12(M,J)+ABARO(M,K)*B11(K,J)
      DO 228 M=1,4
      DO 228 J=1,4
      A11(M,J)=-A12(M,J)+BBAR(M,J)
  228 B11(M,J)=B12(M,J)-CBARO(M,J)
      CALL MATINV(A11,4,BZZ,0,DETERM,IPIVOT,INDEX,4,ISCALE)
      SID=DETERM/ABS(DETERM)
      DO 229 M=1,4
      DO 229 J=1,4
      P(1,M,J)=0.
      DO 229 K=1,4
  229 P(1,M,J)=P(1,M,J)+A11(M,K)*B11(K,J)
      GO TO 250
  224 DO 230 M=1,4
      DO 230 J=1,4
      A11(M,J)=0.
      DO 230 K=1,4
  230 A11(M,J)=A11(M,J)+A1(M,K)*P(I-1,K,J)
      DO 231 M=1,4
      DO 231 J=1,4
  231 A12(M,J)=A11(M,J)+B1(M,J)
      CALL MATINV(A12,4,BZZ,0,DETERM,IPIVOT,INDEX,4,ISCALE)
      SID1=DETERM/ABS(DETERM)
      SIGND=SID*SID1
      SID=SID1
      DO 232 M=1,4
      DO 232 J=1,4
      P(I,M,J)=0.
      DO 232 K=1,4
  232 P(I,M,J)=P(I,M,J)-A12(M,K)*CZ(K,J)
  250 CONTINUE
      DO 235 M=1,4
      DO 235 J=1,4
      A11(M,J)=0.
      B11(M,J)=0.
      DO 235 K=1,4
      A11(M,J)=A11(M,J)+P(K3-1,M,K)*P(K3,K,J)
```

```
235 B11(M,J)=B11(M,J)+BBAR(M,K)*P(K3,K,J)
    DO 236 M=1,4
    DO 236 J=1,4
    A12(M,J)=0.
    DO 236 K=1,4
236 A12(M,J)=A12(M,J)+ABARF(M,K)*A11(K,J)
    DO 237 M=1,4
    DO 237 J=1,4
237 A11(M,J)=A12(M,J)+B11(M,J)+CBARF(M,J)
    CALL DETEV(A11,4,VDET,IPIVOT,4,ISCALE)
    VDET=SIGND*VDET
    WRITE(6,3)VDET,NX,PRES
    IF(ISCALE)239,239,238
239 IF(VDET)240,244,242
242 IF(2-MMM)243,244,243
243 NX=NX+DELNX1
    GO TO 251
240 NX=NX+DELNX2
    MMM=2
    VDEOL=VDET
    GO TO 251
238 NX=NX+DELNX1
    GO TO 251
244 IF(ANXFIN-NX)246,246,253
253 ANXFIN=NX-DELNX2*VDET/(VDET-VDEOL)
    PRESF=PRES-2./R*VDET/(VDET-VDEOL)*DELNX2
    WRITE(6,2)
    WRITE(6,3)ANXFIN,CIRN,PRESF
    WRITE(6,2)
    CIRN=CIRN+1.
    IF(CIRF-CIRN)246,341,341
341 GO TO 252
246 GO TO 100
    END
```

Subroutine for matrix inversion

Subroutine for determinant evaluation

TABLE I

ELASTIC CONSTANTS FOR CORRUGATED CYLINDER

D_x	$\frac{Et_c p^2}{3}(1 - \cos\theta)$
D_y	$\frac{Et_c^3}{12}\left(\frac{1 + \cos\theta}{2}\right)$
D_{xy}	$\frac{Gt_c^3}{12}\left(1 + \frac{2}{1 + \cos\theta}\right)$
E_x	$\frac{2Et_c}{1 + \cos\theta}$
E_y	$\frac{Et_c^3}{4p^2(1 - \cos\theta)}$
G_{xy}	$\frac{Gt_c(1 + \cos\theta)}{2}$
μ'_x	μ
μ'_y	$\mu\frac{E_y}{E_x}$
μ_x	0
μ_y	0

TABLE II

BUCKLING CALCULATIONS FOR AXIAL COMPRESSED RING-

AND STRINGER-STIFFENED ISOTROPIC CYLINDERS

Number of rings	Discrete rings exact prebuckling deformations		Smeared rings exact prebuckling deformations		Discrete rings classical prebuckling deformations		Theory of reference 3	
N	$N_x/E\bar{t}$	n	$N_x/E\bar{t}$	n	$N_x/E\bar{t}$	n	$N_x/E\bar{t}$	n
	Rings-external; stringers-external							
0	0.000851	16	0.000851	16	0.000580	19	0.000580	19
1	.002378*	18	.003144	6	.001340*	25	.001341*	25
2	.002840*	19	.003234	7	.002413*	26	.002412*	26
3	.003198	7	.003508	7	.003615*	18	.003614*	18
4	.003531	6	.003677	6	.004466	7	.004467	7
5	.003761	6	.003820	6	.004629	7	.004629	7
6	.003908	6	.003946	6	.004785	7	.004785	7
7	.004033	6	.004153	5	.004931	5	.004931	5
	Rings-internal; stringers-internal							
0	0.000171	16	0.000171	16	0.000223	15	0.000223	15
1	.000415*	27	.002113	9	.000641*	17	.000641*	17
2	.000678*	62	.002424	8	.001388*	18	.001387*	18
3	.000952*	89	.002623	8	.002444*	19	.002443*	19
4	.001289*	112	.002809	8	.002987	7	.002988	7
5	.001624*	138	.002929	8	.003094	7	.003094	7
6	.002139*	162	.002974	8	.003198	7	.003198	7
7	.002627*	183	.003043	8	.003288	8	.003288	8

*Denotes buckling in panel instability mode

TABLE III

BUCKLING CALCULATIONS FOR AXIAL COMPRESSED

RING-STIFFENED CORRUGATED CYLINDERS

Number of rings	Discrete rings exact prebuckling deformations		Smeared rings exact prebuckling deformations		Discrete rings classical prebuckling deformations		Theory of reference 3	
N	N_x/E_x	n	N_x/E_x	n	N_x/E_x	n	N_x/E_x	n
	Rings-internal							
0	0.000501	0	0.000501	0	0.000501	0	0.000501	0
1	.000957	6	.000976	6	.000972	6	.000976	6
2	.001151	6	.001160	6	.001158	6	.001159	6
3	.001327	6	.001332	6	.001331	6	.001332	6
4	.001495	6	.001499	6	.001498	6	.001499	6
5	.001659	6	.001662	6	.001661	6	.001661	6
6	.001820	6	.001823	6	.001822	6	.001822	6
7	.001980	6	.001982	6	.001981	6	.001981	6
	Rings-external							
0	0.000501	0	0.000501	0	0.000501	0	0.000501	0
1	.001975*	0	.002901	0	.001976*	0	.001976*	0
2	.003262	0	.003365	0	.003365	0	.003365	0
3	.003797	0	.003828	0	.003828	0	.003828	0
4	.004276	0	.004289	0	.004291	0	.004291	0
5	.004743	0	.004749	0	.004754	0	.004754	0
6	.005204	0	.005209	0	.005217	0	.005217	0
7	.005665	0	.005668	0	.005680	0	.005680	0

*Denotes buckling in panel instability mode

TABLE IV

INFLUENCE OF ECCENTRICALLY APPLIED COMPRESSIVE LOADS ON GENERAL INSTABILITY BUCKLING LOADS OF AN INTERNAL RING- AND INTERNAL STRINGER-STIFFENED ISOTROPIC CYLINDER WITH FOUR RINGS

$\frac{\bar{e}}{h}$	$\frac{\hat{N}_x}{E\bar{t}}$	n
0.4	0.002564	10
0.2	.002620	9
0	.002735	9
- 0.2	.002857	9
- 0.5	.003050	9
- 1.0	.003277	8
- 1.2	.003322	8
- 1.3	.003302	7
- 1.5	.003216	6
- 2.0	.003033	6
- 2.5	.002885	6

TABLE V

INFLUENCE OF ECCENTRICALLY APPLIED COMPRESSIVE LOADS

ON BUCKLING LOADS OF STRINGER-STIFFENED ISOTROPIC CYLINDERS

$\frac{\bar{e}}{h}$	$\frac{\hat{N}_x}{E\bar{t}}$	n
Stringers-internal		
1.0	0.000111	17
0	.000171	16
- 1.0	.000298	14
- 2.0	.000489	13
- 3.0	.000618	13
- 4.0	.000649	16
- 5.0	.000630	16
- 6.0	.000599	17
Stringers-external		
2.0	.000220	26
1.5	.000312	24
1.0	.000494	20
.5	.000740	17
0	.000851	16
- .5	.000841	19
- 1.0	.000724	32
- 1.5	.000628	36
- 2.0	.000557	41

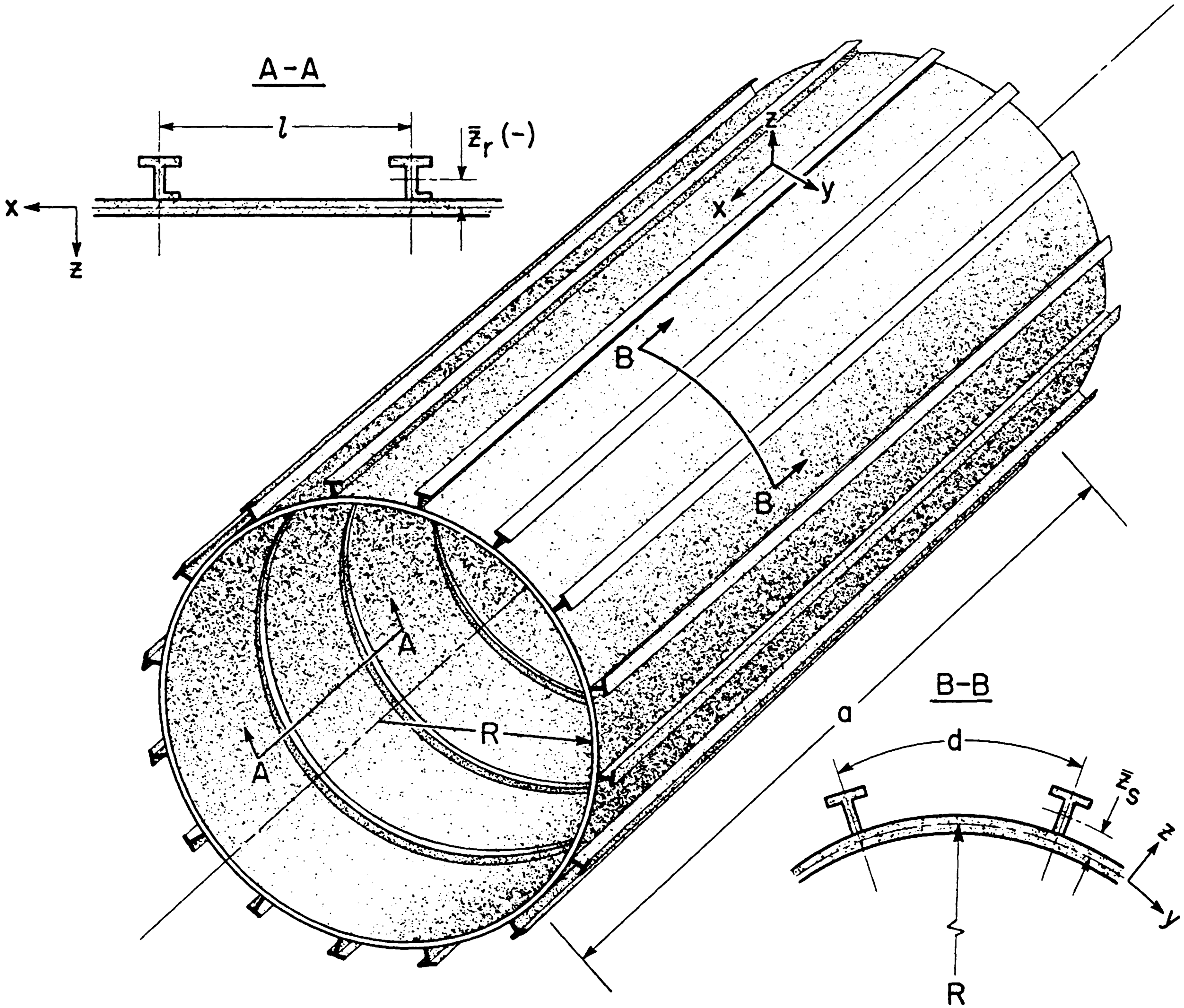

Figure 1.- Geometry of eccentrically stiffened cylinder.

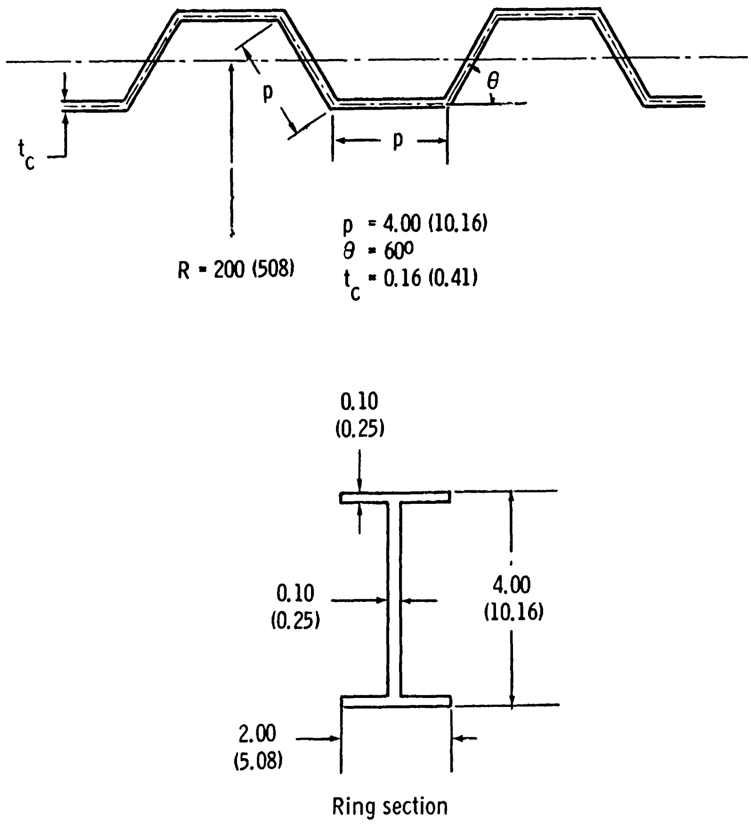

(a) Ring-stiffened corrugated cylinders; a = 200 in. (508 cm).

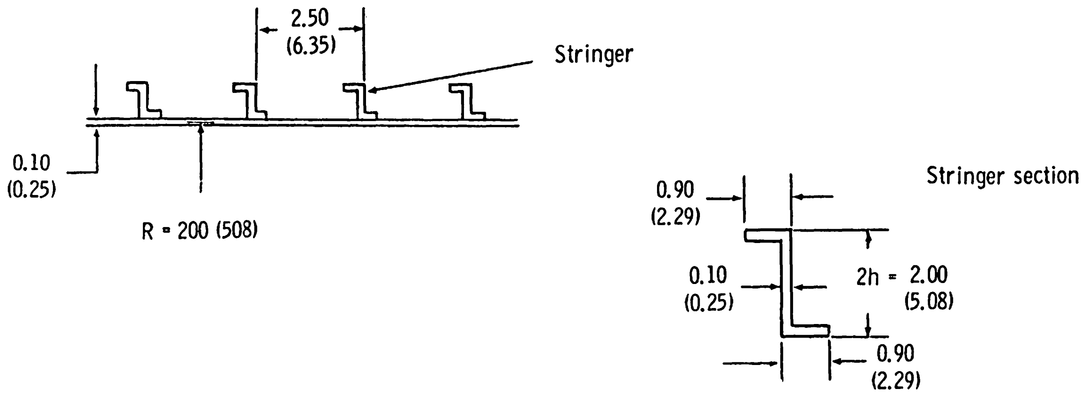

(b) Ring-and-stringer-stiffened cylinders; a = 200 in. (508 cm).
(See fig. 2(a) for ring section.)

Figure 2.- Dimensions of stiffened cylinder. Dimensions are in inches.
(Parenthetical dimensions in cm.)

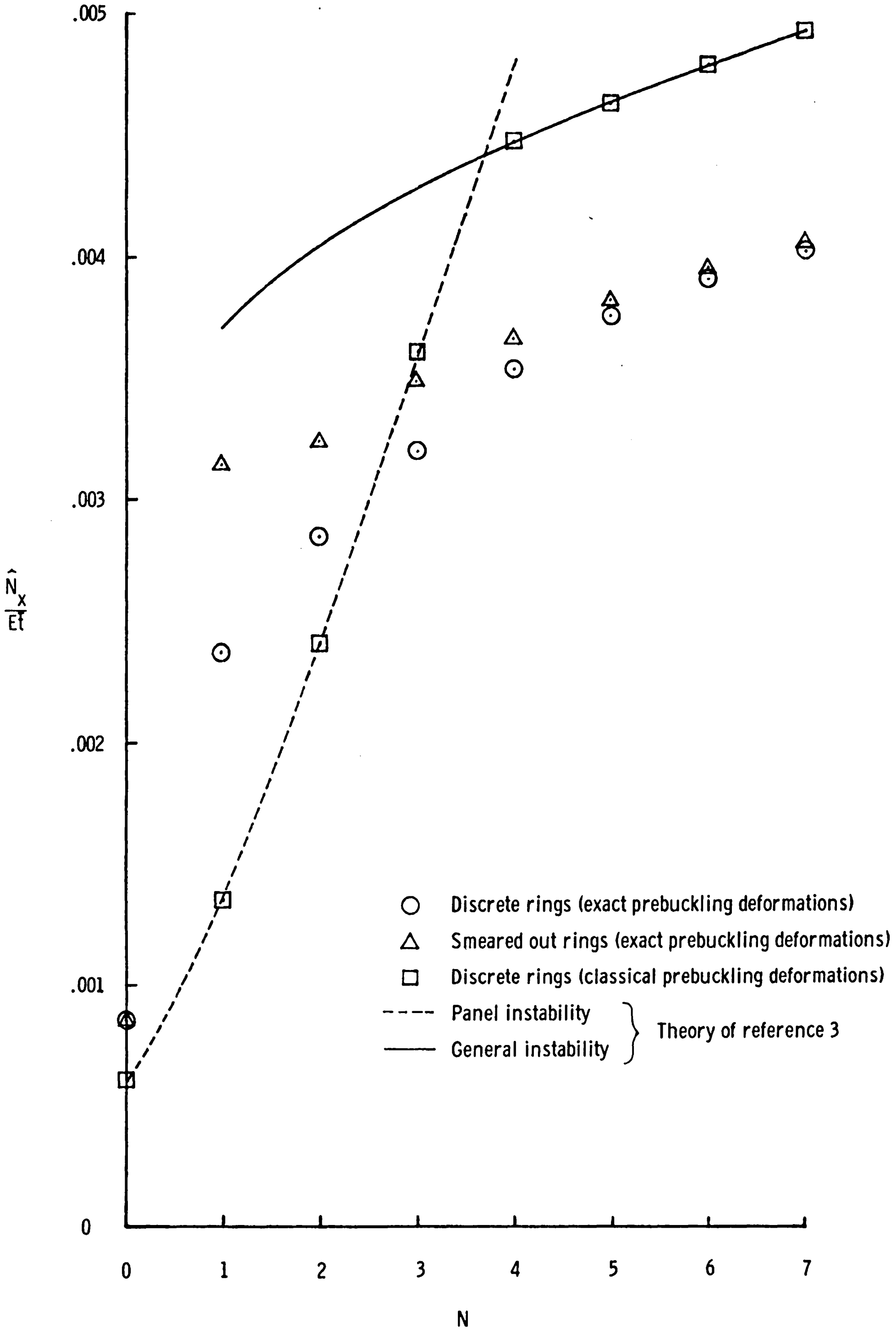

Figure 3.- Buckling predictions for axial compressed external ring- and external stringer-stiffened isotropic cylinders.

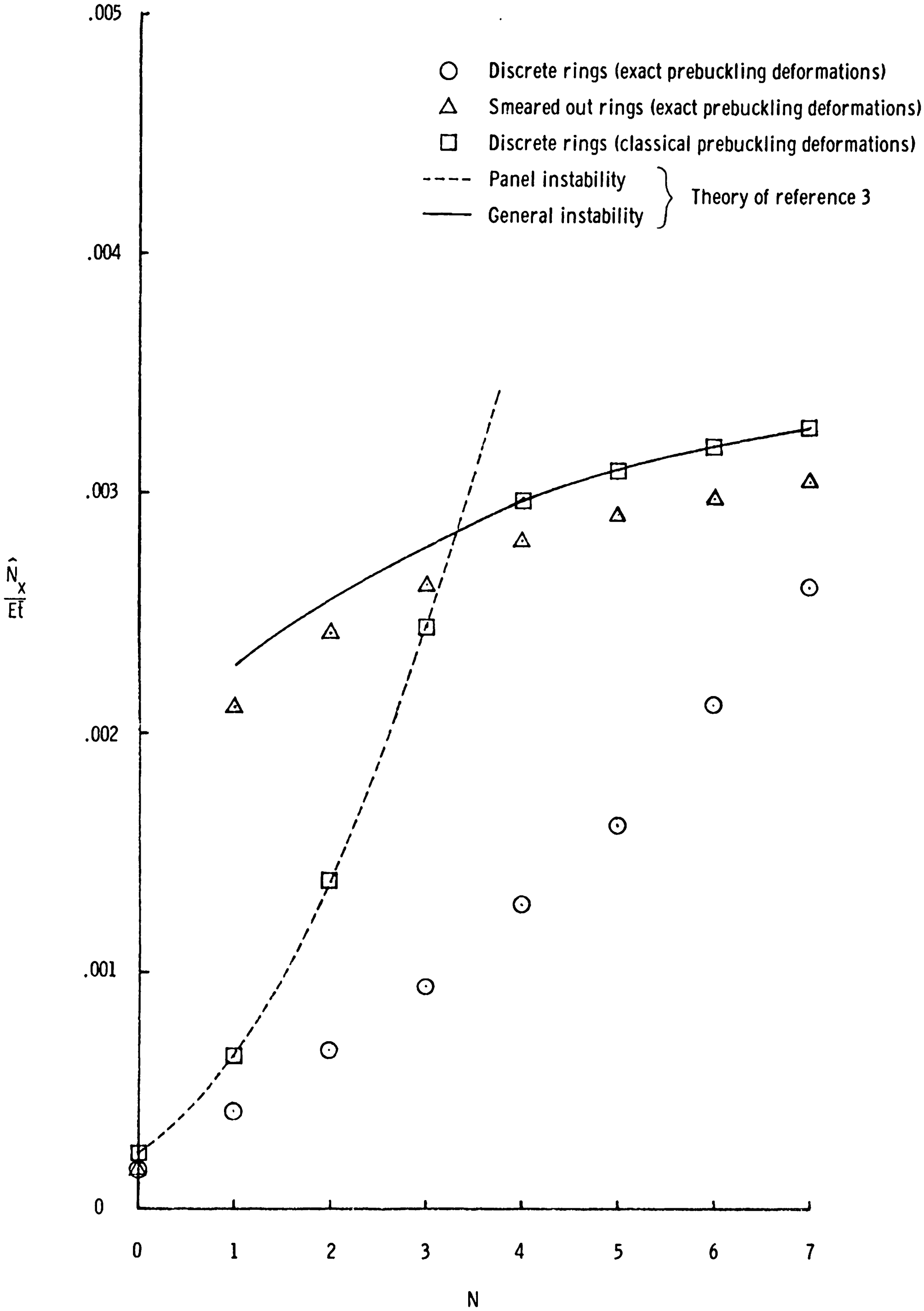

Figure 4.- Buckling predictions for axial compressed internal ring- and internal stringer-stiffened isotropic cylinders.

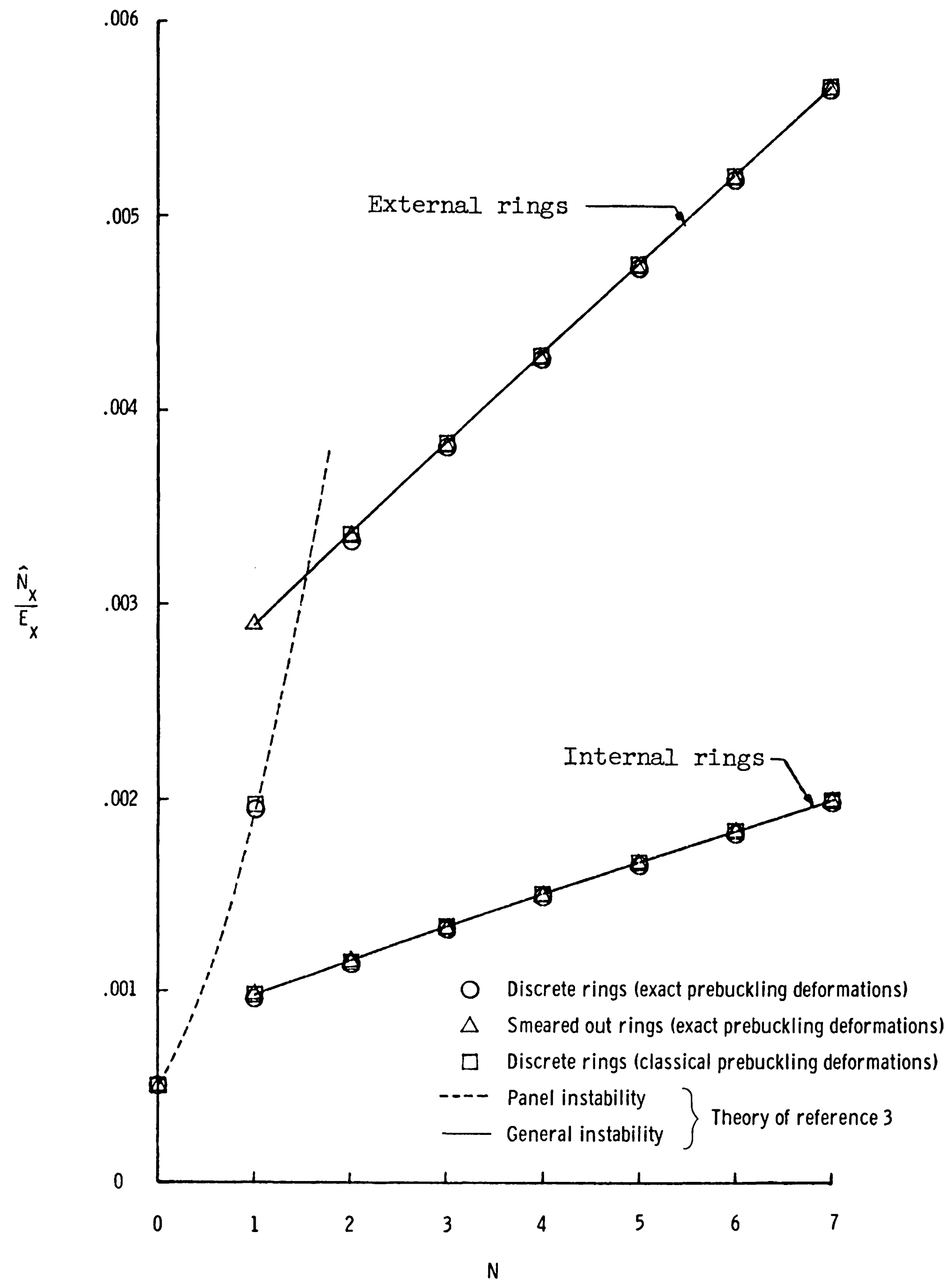

Figure 5.- Buckling predictions for axial compressed ring-stiffened corrugated cylinders.

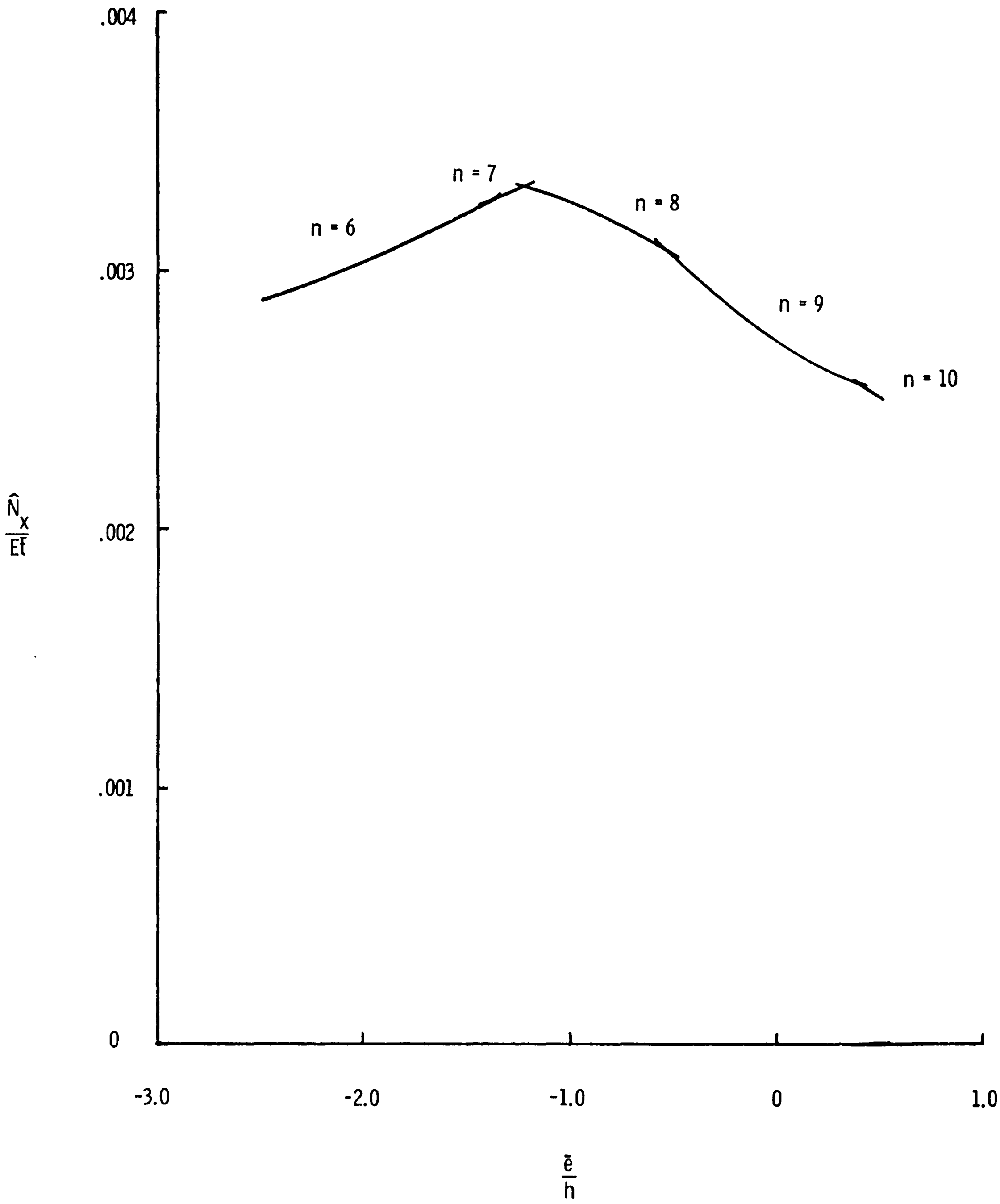

Figure 6.- Influence of eccentrically applied compressive loads on general instability buckling loads of an internal ring- and internal stringer-stiffened isotropic cylinder with four rings.

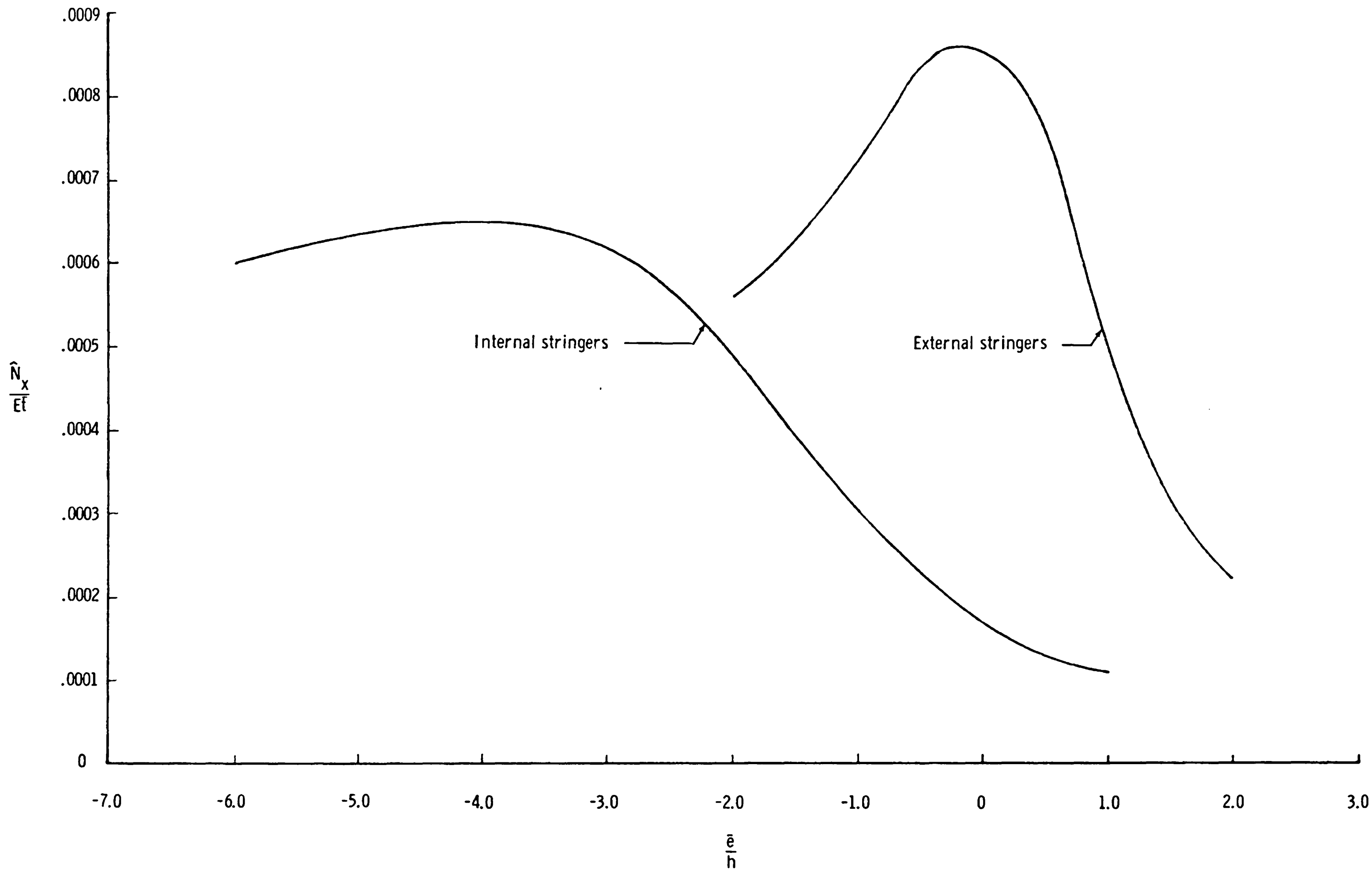

Figure 7.- Influence of eccentrically applied compressive loads on buckling loads of stringer-stiffened isotropic cylinders.

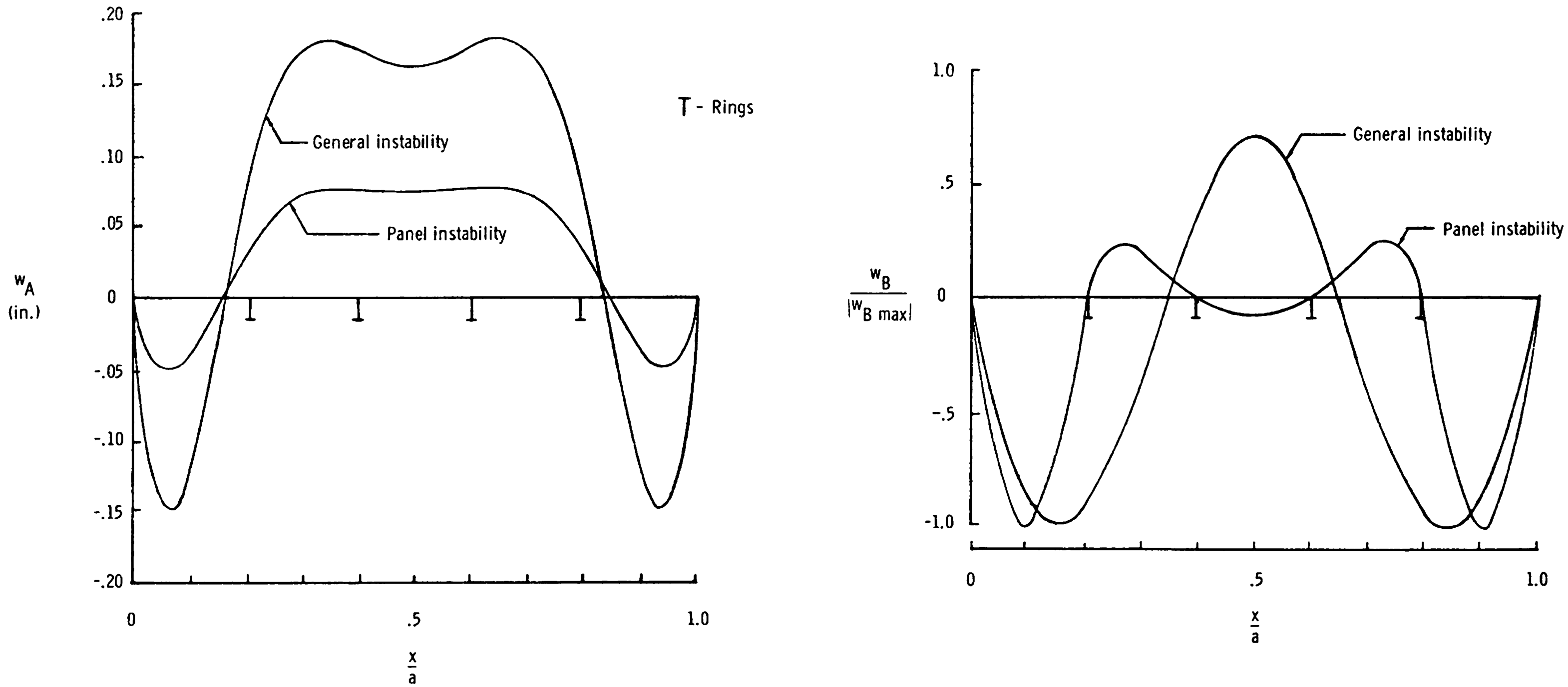

(a) Prebuckling shapes.

(b) Buckling shapes.

Figure 8.- Prebuckling and buckling shapes for panel and general instability buckling modes of an internal ring- and internal stringer-stiffened isotropic cylinder with four rings.

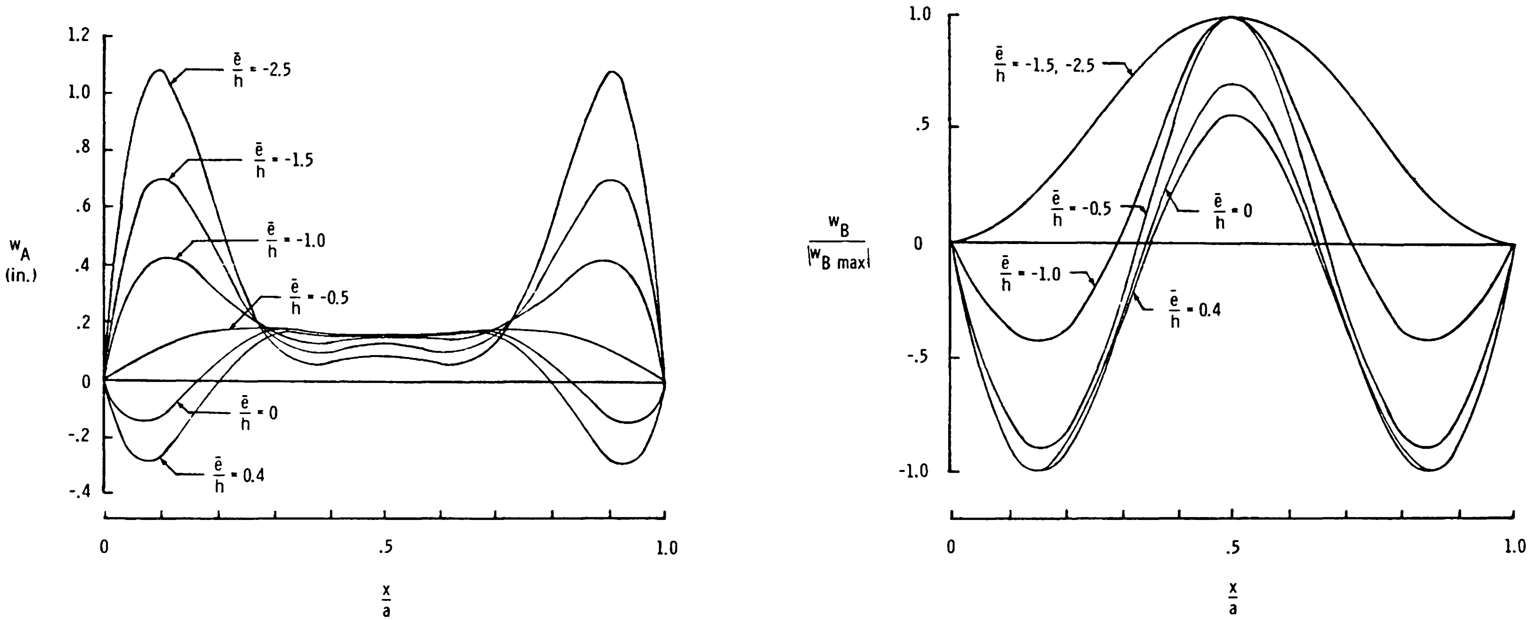

(a) Prebuckling shapes.

(b) Buckling shapes.

Figure 9.- Prebuckling and buckling shapes for internal ring- and internal stringer-stiffened isotropic cylinder with four rings and with eccentrically applied compressive loads.

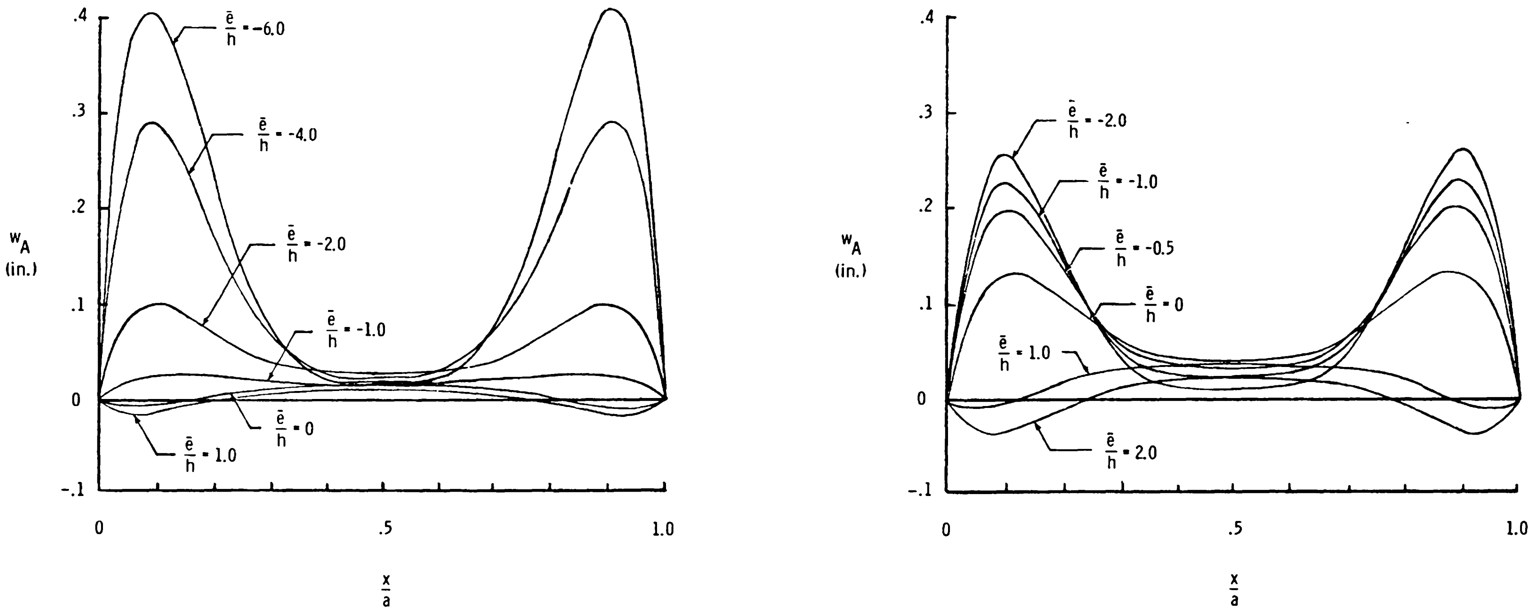

(a) Internal stringers. (b) External stringers.

Figure 10.- Prebuckling shapes for stringer-stiffened isotropic cylinders with eccentrically applied compressive loads.

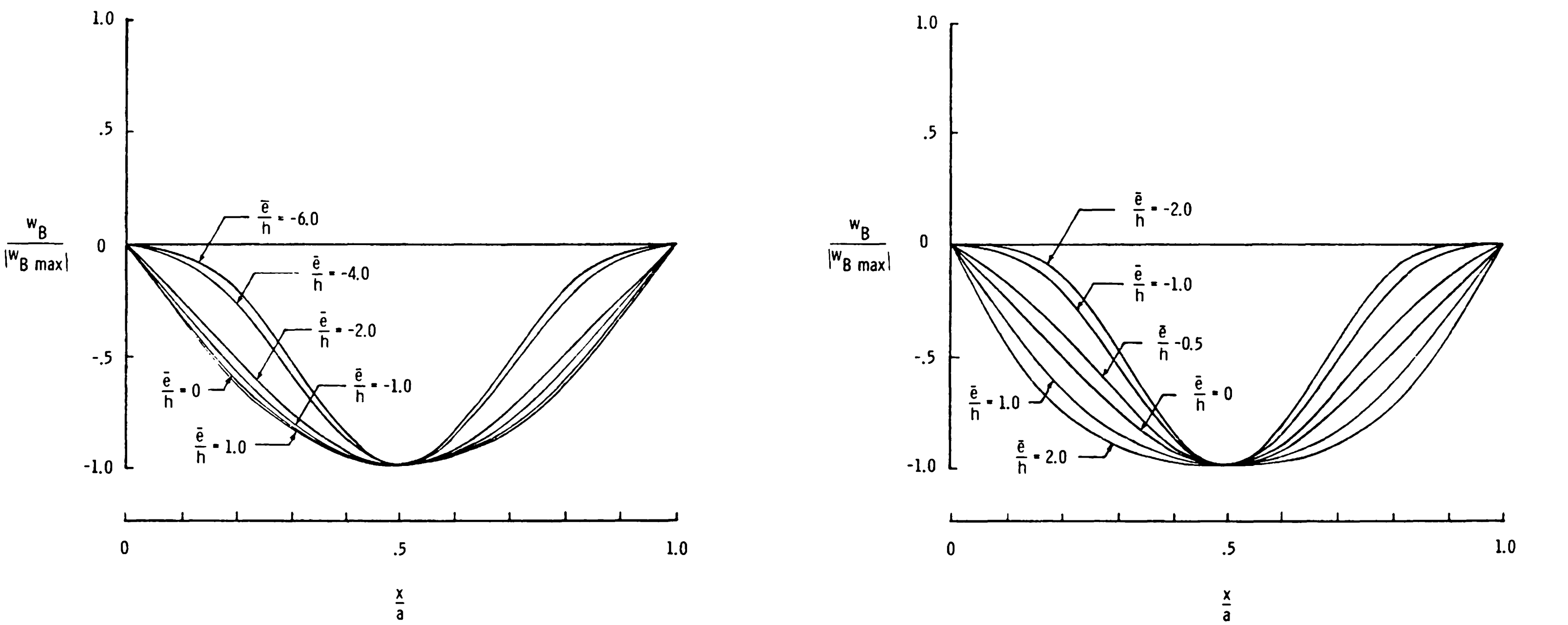

(a) Internal stringers.

(b) External stringers.

Figure 11.- Buckling shapes for stringer-stiffened isotropic cylinders with eccentrically applied compressive loads.

INFLUENCE OF RING STIFFENERS AND PREBUCKLING DEFORMATIONS ON THE BUCKLING OF ECCENTRICALLY STIFFENED ORTHOTROPIC CYLINDERS

By

David L. Block

ABSTRACT

This research presents an analytical investigation of the buckling of eccentrically stiffened orthotropic cylinders and includes the influence of prebuckling deformations. Nonlinear equilibrium equations and boundary conditions are derived by using energy principles. The stiffened cylinder consists of a cylindrical shell made of a homogeneous orthotropic material with eccentric stiffeners on its surface. The rings, or circumferential stiffeners, are considered to be located discretely on circumferential lines along the length of the cylinder and the stringers, or longitudinal stiffeners, are considered to be closely spaced so that their properties can be averaged (smeared out) over the stringer spacing. The stiffeners are considered to be beam elements, to be equally spaced, and to have the stiffener twisting accounted for in an approximate manner. Non-linear Donnell type strain-displacement relations for the shell and the stiffeners are defined and the strain energy of the stiffener-cylinder system is formulated. The governing nonlinear equilibrium equations and boundary conditions are then obtained by the principle of minimum potential energy and the fundamental lemma of calculus of variations. The discrete ring terms are included in the nonlinear equilibrium

equations by use of a Dirac delta function. By a perturbation of the nonlinear equilibrium equations and boundary conditions, a set of nonlinear prebuckling equations and boundary conditions and linear buckling equations and boundary conditions are obtained which govern the prebuckling deformations and stresses and buckling of a stiffened orthotropic cylinder with discrete rings.

Solutions of the prebuckling and buckling equations are obtained for classical simple support boundary conditions and for loadings of axial compression, lateral pressure, and combinations of axial compression and external or internal pressure. The solutions are obtained by the method of finite differences in which the governing equations and boundary conditions are changed to a system of second order differential equations which are then written in terms of finite differences at stations along the length of the cylinder. The difference equations are formulated in terms of a matrix equation which is solved by a modified Gaussian elimination technique. Solutions of the prebuckling and buckling equations for the case where the rings are considered to be smeared out are presented for comparison with the discrete case. A Galerkin solution of the buckling equations for discrete rings assuming classical prebuckling deformations is also presented in the Appendix.

Computed results for two types of contemporary stiffened cylinders are presented in order to study and illustrate the importance of prebuckling deformations, discrete rings, and eccentrically applied compressive loads. The results show that the predicted buckling loads for stiffened cylinders may be substantially affected by using an analysis which takes into account prebuckling deformations.